

# Journal of Visualized Experiments

## Positron Emission Tomography-based Dose Painting Radiation Therapy In A Glioblastoma Rat Model Using The Small Animal Radiation Research Platform --Manuscript Draft--

Article Type:	Methods Article - JoVE Produced Video
Manuscript Number:	JoVE62560R1
Full Title:	Positron Emission Tomography-based Dose Painting Radiation Therapy In A Glioblastoma Rat Model Using The Small Animal Radiation Research Platform
Corresponding Author:	Sam Donche Ghent University Faculty of Medicine and Health Sciences: Universiteit Gent Faculteit Geneeskunde en Gezondheidswetenschappen Ghent, East Flanders BELGIUM
Corresponding Author's Institution:	Ghent University Faculty of Medicine and Health Sciences: Universiteit Gent Faculteit Geneeskunde en Gezondheidswetenschappen
Corresponding Author E-Mail:	sam.donche@ugent.be
Order of Authors:	Sam Donche Jeroen Verhoeven Benedicte Descamps Charlotte Bouckaert Robrecht Raedt Christian Vanhove Ingeborg Goethals
Additional Information:	
Question	Response
Please indicate whether this article will be Standard Access or Open Access.	Standard Access (US\$2,400)
Please specify the section of the submitted manuscript.	Cancer Research
Please indicate the <b>city, state/province, and country</b> where this article will be <b>filmed</b> . Please do not use abbreviations.	Ghent, East-Flanders, Belgium
Please confirm that you have read and agree to the terms and conditions of the author license agreement that applies below:	I agree to the <a href="#">Author License Agreement</a>
Please provide any comments to the journal here.	We were invited to submit an article by Jaydev Upponi
Please indicate whether this article will be Standard Access or Open Access.	Standard Access (\$1400)

**TITLE:**

Positron Emission Tomography-based Dose Painting Radiation Therapy In A Glioblastoma Rat Model Using The Small Animal Radiation Research Platform

**AUTHORS AND AFFILIATIONS:**

Sam Donche<sup>1</sup>, Jeroen Verhoeven<sup>1</sup>, Benedicte Descamps<sup>2</sup>, Charlotte Bouckaert<sup>3</sup>, Robrecht Raedt<sup>3</sup>, Christian Vanhove<sup>2</sup>, Ingeborg Goethals<sup>1</sup>

<sup>1</sup>Department of Diagnostic Sciences, Ghent University, Ghent, Belgium

<sup>2</sup>Department of Electronics and Information Systems, Ghent University, Ghent, Belgium

<sup>3</sup>Department of Head and Skin, Ghent University, Ghent, Belgium

**Email addresses of co-authors:**

Sam Donche	(Sam.Donche@UGent.be)
Benedicte Descamps	(Benedicte.Descamps@UGent.be)
Charlotte Bouckaert	(Charlotte.Bouckaert@UGent.be)
Robrecht Raedt	(Robrecht.raedt@UGent.be)
Christian Vanhove	(Christian.Vanhove@UGent.be)

**Corresponding authors:**

Jeroen Verhoeven	(Jeroen.Verhoeven@UGent.be)
Ingeborg Goethals	(Ingeborg.Goethals@UGent.be)

**KEYWORDS:**Cancer research, small animal irradiation, glioblastoma, magnetic resonance imaging, positron emission tomography, image-guided irradiation, dose-painting-by-numbers, inverse planning

**SUMMARY:**

Here we present a protocol to perform preclinical positron emission tomography-based radiotherapy in a rat glioblastoma model using algorithms developed in-house to optimize the accuracy and efficiency.

**ABSTRACT:**

A rat glioblastoma model to mimic chemo-radiation treatment of human glioblastoma in the clinic was previously established. Similar to the clinical treatment, computed tomography (CT) and magnetic resonance imaging (MRI) were combined during the treatment-planning process. Positron emission tomography (PET) imaging was subsequently added to implement sub-volume boosting using a micro-irradiation system. However, combining three imaging modalities (CT, MRI, and PET) using a micro-irradiation system proved to be labor-intensive because multimodal imaging, treatment planning, and dose delivery have to be completed sequentially in the preclinical setting. This also results in a workflow that is more prone to human error. Therefore, a user-friendly algorithm to further optimize preclinical multimodal imaging-based radiation treatment planning was implemented. This software tool was used to evaluate the accuracy and efficiency of dose painting radiation therapy with micro-irradiation by using an *in silico* study design. The new methodology for dose painting radiation therapy is superior to the previously described method in terms of accuracy, time efficiency, and intra- and inter-user variability. It is

also an important step towards the implementation of inverse treatment planning on micro-irradiators, where forward planning is still commonly used, in contrast to clinical systems.

## INTRODUCTION:

Glioblastoma (GB) is a malignant and very aggressive primary brain tumor. GB is a solid heterogeneous tumor typically characterized by infiltrative boundaries, nuclear atypia, and necrosis<sup>1</sup>. The presence of the blood-brain-barrier and the brain's status as an immune-privileged site makes the discovery of novel targets for chemo- and immunotherapy a daunting task<sup>2-4</sup>. It is noteworthy that the treatment of GB patients has barely changed since the introduction, in 2005, of the Stupp protocol that combines external beam radiation therapy (RT) with concomitant temozolomide, usually followed by adjuvant temozolomide<sup>5</sup>. Typically, the Stupp protocol is preceded by maximal surgical resection. Therefore, alternative treatment approaches are of pivotal importance.

Current radiation therapy for glioblastoma patients delivers a uniform radiation dose to the defined tumor volume. In radiation oncology, there is an important dose-response correlation for glioblastoma with increasing dose, which seems to cap around 60 Gy, due to increased toxicity to the normal brain<sup>6,7</sup>. However, tumors can be very (radiobiologically) heterogeneous, with gradients of oxygen level and/or large differences in cellular density. Metabolic imaging techniques, such as PET, can visualize these biological features and can be utilized to customize the dose prescription. This approach is known as dose painting RT. This term was introduced by Ling et al. in 2000. The authors defined dose painting RT as producing "exquisitely conformal dose distributions within the constraints of radiation propagation and scatter"<sup>8</sup>.

There are two types of dose painting RT, dose painting by contours (DPBC), by which a dose is prescribed to a set of nested sub-volumes, and dose painting by numbers (DPBN), whereby a dose is prescribed at the voxel level. The dose distribution for DPBN RT can be extracted from functional images. The dose in each voxel is determined by the intensity  $I$  of the corresponding voxel in the image, with a lower and upper limit, to make sure that, on the one hand, a sufficient dose is delivered to every part of the tumor. On the other hand, doses do not exceed an upper limit to protect organs at risk and avoid toxicity. The most straightforward method is a linear interpolation (see **Eq. 1**) between minimum dose  $D_{min}$  and maximum dose  $D_{max}$ , proportionally varying between minimum intensity  $I_{min}$  and maximum intensity  $I_{max}$  within the target volume<sup>9,10</sup>:

$$D_I = D_{low} + \frac{I - I_{low}}{I_{high} - I_{low}} (D_{high} - D_{low}) \quad \text{Eq. 1}$$

Because there is some skepticism about the quality assurance of DPBN RT, the deposition of the dose should be verified through preclinical and clinical research<sup>10</sup>. However, only limited data can be acquired from clinical trials, and it has been hypothesized that more insights can be obtained by downscaling to laboratory animals<sup>11,12</sup>. Hence, preclinical studies utilizing precision image-guided radiation research platforms that allow coupling with some very specific techniques, such as autoradiography, are suited for examining open issues and paving the way

towards personalized medicine and novel treatment strategies, such as dose painting RT<sup>13,14</sup>. However, the interpretation of preclinical data must be performed with caution, and drawbacks of these preclinical setups have to be considered<sup>14</sup>.

Micro-irradiation systems, such as the Small Animal Radiation Research Platform (SARRP), are equipped with similar technologies as their clinical counterpart. They include on-board cone-beam CT (CBCT) imaging, a preclinical treatment-planning system (PCTPS), and provide sub-millimeter precision. Clinical dose calculations are performed by inverse treatment planning, whereby one initiates from the desired dose distribution to determine the beams via an iterative algorithm. Preclinical irradiators often use forward planning. In forward planning, the required amount and angle of the beams are selected, and the PCTPS then calculates the dose distribution. The optimization of the plans is performed by manual iteration, which is labor-intensive<sup>15</sup>.

After 2009, novel developments have made the implementation of inverse planning on these research platforms possible<sup>16–18</sup>. To increase the similarity with the clinical method, a motorized variable rectangular collimator (MVC) was developed as a preclinical counterpart of the multi-leaf collimator. A two-dimensional dose painting method utilizing a variable collimator was published by Cho et al.<sup>19</sup>. This research group implemented a three-dimensional (3D) inverse treatment-planning protocol on a micro-irradiator and determined minimum and maximum doses for the target volume and a maximum dose for the organs at risk. These techniques have mainly been evaluated *in silico*, and their preclinical applications need to be explored.

This paper presents an *in silico* study to compare two methodologies for [<sup>18</sup>F]-fluoro-ethyl-L-tyrosine ([<sup>18</sup>F]FET) PET-based dose painting in a GB rat model<sup>20–22</sup> using a small animal radiation research platform. These two methodologies are (1) sub-volume boosting using predefined beam sizes and (2) dose painting using a motorized variable collimator where jaw dimensions are modified based on the PET tracer uptake in the tumor volume. [<sup>18</sup>F]FET is a PET tracer often used in neuro-oncology because of its ability to detect brain tumors<sup>23</sup>. [<sup>18</sup>F]FET is an artificial amino acid that is internalized into tumoral cells but not incorporated into cell proteins. [<sup>18</sup>F]FET uptake corresponds with cell proliferation rate, tumor cell density, and angiogenesis<sup>24</sup>. As this is the most commonly used oncologic brain PET tracer in these authors' institute, this radiotracer was chosen to evaluate the new workflow.

## PROTOCOL:

The study was approved by the local ethics committee for animal experiments (ECD 18/21).

### 1. F98 GB rat cell model

1.1. Culture the F98 GB cells in a monolayer using Dulbecco's Modified Eagle Medium, supplemented with 10% calf serum, 1% penicillin, 1% streptomycin, and 1% L-glutamine, and place them in a CO<sub>2</sub> incubator (5% CO<sub>2</sub> and 37 °C).

1.2. Inoculate the glioma cells into the brain of female Fischer F344 rats (body weight 170 g).

NOTE: Use sterile instruments and wear sterile gloves at all times.

1.2.1. Anesthetize the rats through the inhalation of isoflurane (5% induction, 2% maintenance) mixed with oxygen (0.3 mL/min) through a nose cone. Confirm the anesthetization by the absence of withdrawal reflex of the limb, and immobilize the rats in a stereotactic device using fixation points for the nose and ears. Apply a carbomer eye gel to prevent dry eyes under anesthesia. Maintain the body temperature by a thermoregulated heating pad and rectal probe at 37 °C.

1.2.2. Shave the rat from the eye level to the back of the skull, and disinfect the skin with isobetadine. Inject xylocaine (with adrenaline 1:200000, 0.1 mL) subcutaneously for local anesthesia.

1.2.3. Expose the skull through a midline scalp incision and make a small hole with a drill tool 3 mm posterior and 3 mm lateral to the bregma in the right hemisphere.

1.2.4. Insert a stereotactically guided insulin needle (29 G) and inject 5 µL of cell suspension (20,000 F98 GB cells) 3 mm deep using a microsyringe pump controller. Leave the needle in place for 5 min, giving the cell suspension time to diffuse into the tissue.

1.2.5. Withdraw the syringe slowly and close the hole in the skull with bone wax. Suture the skin (polyamide 6, thickness 4-0) and inject meloxicam subcutaneously (1 mg/kg, 2 mg/mL). Apply xylocaine gel.

1.2.6. Stabilize the body temperature of the animal post-surgery using a red lamp. Monitor the awakening of the rat until it has regained sufficient consciousness. Do not return the animal to the company of other animals until fully recovered. House all animals under environmentally controlled conditions (12 h light/dark cycle, 20–24 °C, and 40–70% relative humidity) with food and water *ad libitum*.

1.2.7. Be sure to monitor the animals daily and maintain a daily health status log by checking their body weight, food, water intake, and their activity and behavior. Use a lethal dose of pentobarbital sodium to euthanize the animals (160 mg/kg) if a decline of 20% body weight is observed or when the normal behavior severely deteriorates (e.g., lack of grooming).

## **2. Confirmation of tumor growth**

2.1. Evaluate tumor growth 8 days post-inoculation. Anesthetize the rats through the inhalation of isoflurane (5% induction, 2% maintenance) mixed with oxygen (0.3 mL/min) through a nose cone. Confirm the anesthetization by the absence of withdrawal reflex of the limb.

2.2. Inject a gadolinium-containing contrast agent (0.4 mL/kg) through an intravenously placed tubing in the lateral tail vein. Cover the animal with a heated blanket and place them in the MRI bed. Apply a carbomer eye gel to prevent dry eyes under anesthesia. Place the MRI bed

in the holder with a Tx/Rx Rat brain volume coil.

2.3. Perform a localizer scan followed by a T<sub>2</sub>-weighted spin-echo scan to assess tumor growth. Use these T<sub>2</sub>-MRI sequence settings: repetition time (TR)/echo time (TE) 3661/37.1 ms, 109 μm isotropic in-plane resolution, slice thickness 600 μm, 4 averages, 30 slices, total acquisition time (TA) 9 min 45 s.

2.4. If a tumor is confirmed on the T<sub>2</sub>-weighted acquisition, perform a T<sub>1</sub>-weighted contrast-enhanced spin echo scan. Use these T<sub>1</sub>-MRI sequence settings: TR/TE 1539/9.7 ms, 0.117 mm isotropic in-plane resolution, slice thickness 600 μm, 3 averages, 30 slices, TA 4 min 15 s.

2.5. After the MRI, continuously supervise the animal until it regains full consciousness.

2.6. When the tumor reaches a diameter of 7 to 8 mm, usually observed 12 days after inoculation, select the animal for therapy.

### **3. Multimodality imaging of target volume selection**

NOTE: PET/MRI-guided irradiation requires the sequential acquisition of a multimodal dataset. After intravenous administration of the radiotracer, PET imaging is started, followed by contrast-enhanced T<sub>1</sub>-weighted MRI and finally a treatment-planning CT.

3.1. Anesthetize the animal with isoflurane (5% induction, 2% maintenance) mixed with oxygen (0.3 L/min) using a nose cone. Confirm anesthetization when the rats do not exhibit any withdrawal reflex of the limb. Apply carbomer eye gel to prevent dry eyes under anesthesia.

3.2. Insert the tubing intravenously in the lateral tail vein, enabling the injection of 10–12 MBq of PET radioactive tracer dissolved in 200 μL of saline. Inject [<sup>18</sup>F]-FET, 1 h before PET acquisition. Let the animal regain consciousness while the tracer is distributed through the body.

3.3. Anesthetize the animal again, as described in step 3.1. Place the animal on a multimodality bed (here, made in-house) and secure it using hook-and-loop fasteners, maintaining a fixed position during the imaging and micro-irradiation. Fix a capillary filled with the MRI/PET agent (see the **Table of Materials**) for easier co-registration. Wrap the animal in bubble wrap to preserve its body temperature during the multimodality imaging and therapy.

3.4. Perform a PET scan 1 h after the injection of the PET tracer. Reconstruct the PET scan into a 3D volume (192 x 192 x 384 matrix) with 0.4 mm voxel size by applying a Maximum-Likelihood Expectation-Maximization (MLEM)-algorithm using 30 iterations.

NOTE: A dedicated PET scanner for laboratory animal imaging was used with an axial field of view of 130 mm and a bore diameter of 72 mm. This system provides sub-mm (0.85 mm) spatial resolution.

3.5. Inject an MRI contrast agent (0.4 mL/kg) intravenously into the tail vein. Place the rat, still fixed on the multimodality bed, in the animal holder of the MRI scanner (**Table of Materials**). Perform a localizer scan followed by a contrast-enhanced T<sub>1</sub>-weighted spin-echo sequence, analogous to step 2.4.

3.6. Place the animal, still fixed on the multimodality bed, on a plastic holder secured onto the four-axis robotic positioning table on the micro-irradiator. Perform a high-resolution treatment-planning cone-beam CT using a tube voltage of 70 kV, a tube current of 0.4 mA, a 1 mm aluminum filter, and a 20 x 20 cm (1024 x 1024 pixel) amorphous Si flat panel detector. Acquire a total of 360 projections over 360°. Reconstruct the CT images with an isotropic voxel size of 0.275 mm (411 x 411 x 251 matrix).

#### 4. Image co-registration

NOTE: The co-registration is performed with a semi-automatic MATLAB code developed in-house. The code can be found on Github at <https://github.com/sdonche/DosePainting>. The different steps are described below.

4.1. Place the three image modalities ([<sup>18</sup>F]FET PET, contrast-enhanced T<sub>1</sub>-weighted MRI, and cone-beam CT) into one folder. Convert DICOM images to the **NIfTI format** using the **dcm2niix** function from the **mricon image viewer**<sup>24</sup>.

4.2. Import the converted images into MATLAB and filter the PET image with a Gaussian filter using a **Full-Width Half-Max (FWHM) of 1 mm**.

4.3. Reorient the images so that the cartesian axes from all imaging modalities correspond with each other.

NOTE: For this setup, the CT image was flipped around the Y-axis; the MRI was flipped around the X-axis, and the PET was flipped around the Y-axis.

4.4. Crop the PET image to simplify automatic co-registration.

NOTE: For this setup, 40 pixels were set to zero from both sides of the X-axis (left and right of the animal); on the dorsal and ventral side of the animal (Y-axis), 60 and 40 pixels were set to zero, respectively; along the longitudinal axis (or Z-axis), 170 and 30 pixels are set to zero for inferior and superior side, respectively.

4.5. Move the image centers close to each other to simplify automatic co-registration.

4.6. Perform the actual rigid-body co-registration using Statistical Parametric Mapping (SPM) in MATLAB<sup>26</sup>. Use the following registration parameters (others on default): objective function: mutual information; separation: [4 1 0.2]; tolerances: [0.02 0.02 0.02 0.001 0.001 0.001 0.01 0.01 0.01 0.001 0.001 0.001]; histogram smoothing: [1 1]; interpolation: trilinear.

## 5. Radiation treatment planning

NOTE: A MATLAB app and multiple MATLAB scripts were written for the radiation treatment planning. The code can be found on Github at <https://github.com/sdonche/DosePainting>. The different steps are explained below.

### 5.1. Method 1

5.1.1. Load the three different imaging modalities into the MATLAB app. Place a generous bounding box around the contrast enhancement on the T<sub>1</sub>-weighted MRI scan (**Figure 1**). Determine the contrast-enhanced volume using a threshold (**Figure 2**). If multiple regions have been selected, select only the largest volume, the center of which is considered as the first isocenter to deliver a prescribed dose for RT (**Figure 3**).

5.1.2. Expand the previously determined MRI contrast enhancement by 10 pixels in each direction. If multiple regions are detected, retain only the largest PET volume, the center of which is considered the second isocenter to deliver a prescribed dose for RT.

NOTE: In this PET volume, the PET boost volume is defined by the pixels with a higher signal intensity than  $0.90 \times$  maximal signal intensity (in the bounding box) in this volume.

5.1.3. Use the following irradiation settings for the calculated isocenters (**Figure 4** and **Table 1**).

5.1.3.1. For the first isocenter (MRI), give a prescribed dose of 2000 cGy using 3 non-coplanar arcs at couch positions 0°, -45°, and -90° with a gantry rotation of 120°, 120°, and 60°, respectively. Use a fixed collimator size of 10 x 10 mm, but use an appropriate collimator (e.g., a 5 x 5 mm collimator) when smaller tumor sizes need to be irradiated. Be careful in considering the animal's welfare when the tumor volumes are larger than 10 mm.

5.1.3.2. For the second isocenter (PET), give a prescribed dose of 800 cGy using 3 non-coplanar arcs at couch positions 0°, -45°, and -90° with a gantry rotation of 120°, 120°, and 60°, respectively. Use a fixed collimator size of 3 x 3 mm.

5.1.4. Calculate the dose distribution within the animal and the beam delivery parameters.

### 5.2. Method 2

5.2.1. Load the three different imaging modalities into the MATLAB app. Place a generous bounding box around the contrast-enhancement on the [<sup>18</sup>F]FET PET image, analogous to step 5.1.1.

5.2.2. Determine the volumes defined by the pixels with a signal intensity higher than  $A \times$  maximal signal intensity (in the aforementioned bounding box), with A equal to 0.50, 0.60, 0.70,



0.80, and 0.90. Name these volumes V50, V60, V70, V80, and V90, respectively.

5.2.3. Determine the isocenters and the jaw dimensions for each beam required to guide the motorized variable collimator using the MATLAB script (see **Figure 5**).

5.3.3. Use the following settings for the calculated isocenters and jaw dimensions:

5.3.3.1. For V50, give a prescribed dose of 2000 cGy distributed over 16 beams (each 125 cGy; couch and gantry positions in **Table 2**). Use the calculated jaw dimensions for the MVC.

NOTE: Here, an additional margin of 1 mm has been included to account for microscopic tumor infiltration.

5.3.3.2. For V60–V90, give a prescribed dose of 800 cGy distributed over 40 beams (each 20 cGy; couch and gantry positions in **Table 2**). Use the calculated jaw dimensions for the MVC.

5.3.4. Calculate the dose distribution within the animal and the beam delivery parameters.

## 6. Plan evaluation

NOTE: To compare the two methods, calculate the dose-volume histograms (DVH) and Q-volume histogram (QVH) in the V50 PET volume. Here, a MATLAB script, developed in-house, was used. The code can be found on Github at <https://github.com/sdonche/DosePainting>.

### 6.1. Dose-volume histogram

6.1.1. Generate DVH from the dose distribution that was obtained from the SARRP.

6.1.2. Determine the maximum, mean, and minimum doses from the DVH by calculating the  $D_{10}$ ,  $D_{50}$ , and  $D_{90}$ , where  $D_x$  stands for the dose received by  $x\%$  of the volume.

### 6.2. Q-volume histogram

6.2.1. Calculate an ideal dose for every pixel using **Eq. 1**, which is a linear interpolation between the minimum and maximum doses, proportionally varying between the minimum PET intensity and maximum PET intensity within the target volume to give an ideal dose map.

6.2.2. Calculate the Q-value  $Q_p$  for every pixel using the following equation (**Eq. 2**):

$$Q_p = \frac{D_p}{D_i} \quad \text{Eq. 2}$$

With  $D_p$  being the dose obtained by planning and  $D_i$ , the dose objective for planning.

6.2.3. Generate QVH from the obtained Q-values.

6.2.4. Calculate the quality factor (Q-factor,  $Q_F$ ) to evaluate the difference between the planned and intended doses using **Eq. 3**:

$$Q_F = \frac{1}{n} \sum_{p=1}^{p=n} |Q_p - 1| \quad \text{Eq. 3}$$

## REPRESENTATIVE RESULTS:

The feasibility of PET- and MRI-guided irradiation in a glioblastoma rat model using the SARRP to mimic the human treatment strategy has been previously described<sup>20–22</sup>. While the animal was fixed on a multimodality bed made in-house, it was possible to create an acceptable radiation treatment plan combining three imaging modalities: PET, MRI, and CT. In these methods, an external software package (see the **Table of Materials**) was used to co-register the images using rigid-body transformations manually. The contrast-enhanced T<sub>1</sub>-weighted MRI and PET images were visually assessed from which the isocenters were manually selected. However, this methodology proved to be labor-intensive and certainly has an impact on the animals as they have to stay under general anesthesia during the multimodality imaging and the creation of a treatment plan. Therefore, the new methodology aims to automate specific steps in this process to reduce the overall variance and time required to create a radiation treatment plan.

In this paper, two methodologies are compared. Method 1 is very similar to the previously published methodology<sup>20–22</sup> with a few adjustments (**Table 1**). However, in contrast to the previously published methodology, most of the process is automated using a MATLAB code developed in-house. Method 2 is a more sophisticated method in which a series of isocenters and jaw dimensions for the MVC will be determined based on the [<sup>18</sup>F]FET PET uptake (**Figure 5**). The isocontours for V50, V60, V70, V80, and V90 are shown in **Figure 6**.

Both methods were applied to three different cases (**Figure 7**). These cases can be divided into two different types: [<sup>18</sup>F]FET PET uptake in the infiltrative tumor front and the presence of tumor necrosis and [<sup>18</sup>F]FET PET uptake indicating no tumor necrosis. Case 1 can be described as a spherical homogeneous PET uptake, while Cases 2 and 3 have a ring-shaped uptake where the reduced PET-uptake is most likely necrotic tissue. Case 3 also shows an additional region growing out towards the dorsal region.

After calculating the setup parameters for both methods, the dose distributions for each case (**Figure 8**) were determined using the SARRP's PCTPS. The DVHs (**Figure 9**) can be obtained from the dose distributions in the volumes defined by the pixels with signal intensity higher than 0.50 × maximal PET signal intensity (in the bounding box). One can observe that the DVHs for Method 2 are systematically closer to the ideal dose distribution than those for Method 1. A substantial tumor volume receives insufficient irradiation in Cases 2 and 3 when treated with Method 1. **Table 3** confirms these conclusions: the D<sub>90</sub> and D<sub>50</sub> values are considerably lower for Method 1 than for Method 2. The QVHs (**Figure 10**) can also be obtained from these dose distributions.

Ideally, these curves make a sharp drop at a Q-value equal to one. Method 2 always results in dose distributions that are closer to the dose objective. **Table 4** also demonstrates superior overall Q-factors for Method 2. The minimal dose ( $D_{90}$ ) of 2000 cGy has been achieved for all cases with Method 2, while it was not achieved with Method 1 in 2 cases. This means that the tumor volume received insufficient irradiation using Method 1.

#### FIGURE AND TABLE LEGENDS:

**Figure 1: Bounding box placement.** The  $T_1$ -weighted contrast enhancement is visible in the F98 GB rat model, and a generous bounding box is placed around the tumor using the MATLAB code developed in-house.

**Figure 2:  $T_1$ -weighted contrast-enhancing tumor delineation: step 1.** The tumor volume is delineated on the contrast-enhanced  $T_1$ -weighted MRI using thresholding. Abbreviation: MRI = magnetic resonance imaging.

**Figure 3:  $T_1$ -weighted contrast-enhancing tumor delineation: step 2.** If multiple volumes are detected during the thresholding step, the largest volume is retained for further processing.

**Figure 4: Isocenter calculation for Method 1.** Contrast-enhanced  $T_1$ -weighted MRI, CT, and PET images are depicted. The blue and red circles represent the MRI- and PET-based isocenters, respectively. Abbreviations: MRI = magnetic resonance imaging; CT = computed tomography; PET = positron emission tomography.

**Figure 5: Explanation of jaw setup calculation.** Step 1: the tumor volume is determined (blue dots, top image). Step 2: a plane (black grid) is created perpendicular to the incident beam (magenta line, top image) at specific couch and gantry positions. Step 3: the tumor voxels (blue dots, top image) are perpendicularly projected onto the aforementioned plane, resulting in a set of projected voxels (red dots). Step 4: determine the isocenter and jaw dimensions (green lines, bottom image) so that all the projected voxels are included within the rectangular beam defined by the two symmetrical jaws of the variable collimator (bottom image). These figures were generated in MATLAB.

**Figure 6: Tumor isocontours.** Transaxial, coronal, and sagittal slices through the brain tumor with tumor volumes V50, V60, V70, V80, and V90 determined by the isocontours corresponding to 50%, 60%, 70%, 80%, and 90% of the maximum tumor uptake in the PET images. Abbreviations: TV = transaxial; COR = coronal; SAG = sagittal; PET = positron emission tomography.

**Figure 7: [ $^{18}\text{F}$ ]FET PET imaging for the three cases.** The sagittal, transverse, and frontal views are displayed for all three cases.

**Figure 8: Dose distributions for both methods.** Sagittal, transverse, and frontal views for all three cases are displayed for both Method 1 and Method 2. The dose distribution is shown together with the cone-beam CT imaging from the SARRP. Abbreviations: CT = computed tomography;

SARRP = small animal radiation research platform.

**Figure 9: DVH curves for all cases.** DVH curves (in cGy) are shown for Method 1, Method 2, and the Ideal Dose Map. Abbreviation: DVH = dose-volume histogram.

**Figure 10: Q-volume histogram for all cases.** QVH curves are shown for Method 1, Method 2, and the Ideal Dose Map. Ideally, the calculated QVH must have a sharp drop at Q-value = 1 (Ideal dose map, blue line). Abbreviation: QVH = Q-volume histogram.

**Table 1: Method comparison.** This table further clarifies Method 1, Method 2, and the Previous Method (referring to the method that has already been published)<sup>20–22</sup>. Methods 1 and 2 utilize a preclinical PET scanner<sup>27</sup> with sub-millimeter spatial resolution, making it possible to visualize the tumor heterogeneity more clearly. At couch position -90°, it is only possible to use 60° out of 120° to avoid collision with the animal. Despite this drawback, this couch position has easier access to the tumor because it is situated in the right hemisphere. The other couch positions can make the full 120° rotations. Abbreviations: CE T<sub>1</sub> = contrast-enhanced T<sub>1</sub>-weighted; MVC = motorized variable collimator; PET = positron emission tomography.

**Table 2: Beam setup for Method 2.** The gantry and couch positions of all the different beams are displayed. V50 uses all configurations, whereas V60–V90 only use the configurations shown in bold.

**Table 1: DVH values.** D<sub>10</sub>, D<sub>50</sub>, and D<sub>90</sub> were calculated as substitutes for maximum, mean, and minimal doses, respectively. D<sub>x</sub> stands for the dose received by x% of the volume. Abbreviation: DVH = dose-volume histogram.

**Table 2: Q-factors.** The table displays the overall Q-factors for Method 1 and Method 2 for each case. The Q-factor will be zero if the delivered dose and prescribed dose are equal.

## DISCUSSION:

A rat GB model to mimic the chemo-radiation treatment in the clinic for glioblastoma patients was previously described<sup>20</sup>. Similar to the clinical method, CT and MRI were combined during the treatment-planning process to obtain more precise irradiation. A multimodality bed to minimize (head) movement was used when the animal was moved from one imaging system to another. Subsequently, PET imaging was added to the treatment-planning process, and PET-based sub-volume boosting could be successfully implemented<sup>21,22</sup>. The inclusion of a functional image modality, such as PET, in the treatment-planning process allows the visualization of the (biological) tumor heterogeneity. This facilitates the targeting of aggressive and/or radiation-resistant tumor regions. Although this method is feasible, it proved to be very labor-intensive because multimodal imaging, treatment planning, and dose delivery must be completed sequentially in a preclinical setting. Moreover, during this process, the animals have to stay under general anesthesia<sup>22</sup>. Therefore, it is essential to improve the efficiency of the preclinical treatment-planning process.

This paper presents a user-friendly semi-automatic algorithm to further optimize preclinical multimodal imaging-based radiation treatment planning. Co-registration between planning CT, MRI, and PET were automated, in combination with the detection of the target isocenters. Of note, the software tool should not be considered as a black box, and it is crucial to perform proper quality checks. The most critical step in this entire process is to evaluate the results of the automatic co-registration of planning CT, MRI, and PET that should be as accurate as possible. The output of the algorithm consists of the positions of the target isocenters and the jaw dimensions of the MVC for the different radiation beams. These values can be imported into the most recent version of the PCTPS.

This software tool was used to evaluate the accuracy and efficiency of PET-based dose painting on the micro-irradiator by using an *in silico* study design. The optimized treatment-planning process was superior to the previously described method<sup>21,22</sup> in terms of time efficiency, intra- and inter-user variability, and accuracy. While conventional preclinical treatment planning, including multimodal imaging, can require up to 180 min<sup>22</sup>, this time could be reduced to ~80 min with both the semi-automatic methods presented in this manuscript. Moreover, human errors are more likely in the conventional treatment-planning process during manual co-registration and visual determination of the isocenters, resulting in larger intra- and inter-user variability. The automatic co-registration and detection of the target isocenters by the algorithm will reduce these intra- and inter-user variabilities. In addition, the optimized and automated workflow provides more accurate irradiation of the tumor volume. This is illustrated by the lower Q-factors (**Table 4**), which assesses the difference between the dose calculated/delivered by the PCTPS and the prescribed dose.

It is also noteworthy that the use of an MVC results in a reduced dose to the surrounding normal brain tissue, compared to collimators with a fixed beam size. This is illustrated in **Figure 7** and is important to narrow the gap between clinical trials evaluating DPBN RT strategy (where multi-leaf collimators are used) and laboratory animal radiation research. However, we assume that dose delivery might be slightly slower when using an MVC to switch between beam positions and adjust the jaw dimensions for each individual beam. Finally, preclinical treatment planning is most often done by forward planning. The methodology described in this paper is a crucial step towards inverse planning, which is generally used in the clinic, and further narrows the gap between preclinical radiation research and the clinic.

This study also has some limitations. For the experiments described in this manuscript, the most commonly used amino acid PET tracer [<sup>18</sup>F]FET was used. When using other PET tracers to guide radiation treatment, the semi-automatic workflow should be properly examined because co-registration might be less accurate. Further, the impact of using a different voxel size for PET and/or MRI on treatment planning and dose delivery should be further investigated. In conclusion, the methodology described here to optimize the preclinical treatment-planning process has many advantages compared to the previously described method<sup>21,22</sup>. Using an *in silico* study design, it was proven that the novel workflow for preclinical multimodal treatment planning is more accurate in terms of dose delivery, more time-efficient, and shows less intra- and inter-user variability. These improvements are essential to narrow the gap between clinical

and preclinical radiation research and for the development of new therapeutics and/or radiation therapy procedures for glioblastoma.

#### **ACKNOWLEDGMENTS:**

The authors would like to thank Lux Luka Foundation for supporting this work.

#### **DISCLOSURES:**

The authors have no conflicts of interest to disclose.

#### **REFERENCES:**

1. Louis, D. N. et al. The 2016 World Health Organization classification of tumors of the central nervous system: a summary. *Acta Neuropathologica*. **131** (6), 803–820 (2016).
2. Wadajkar, A. S. et al. Tumor-targeted nanotherapeutics: Overcoming treatment barriers for glioblastoma. *Wiley Interdisciplinary Reviews. Nanomedicine & Nanobiotechnology*. **9** (4), 10.1002/wnan.1439 (2016).
3. Lim, M., Xia, Y., Bettegowda, C., Weller, M. Current state of immunotherapy for glioblastoma. *Nature Reviews. Clinical Oncology*. **15** (7), 422–422 (2018).
4. McGranahan, T., Li, G, Nagpal, S. History and current state of immunotherapy in glioma and brain metastasis. *Therapeutic Advances in Medical Oncology*. **9** (5), 347–368 (2017).
5. Stupp, R. et al. Radiotherapy plus concomitant and adjuvant temozolomide for glioblastoma. *The New England Journal of Medicine*. **352** (10), 987–996 (2005).
6. Von Neubeck, C., Seidlitz, A., Kitzler, H. H., Beuthien-Baumann, B., Krause, M. Glioblastoma multiforme: Emerging treatments and stratification markers beyond new drugs. *The British Journal of Radiology*. **88** (1053), 20150354 (2015).
7. Mann, J., Ramakrishna, R., Magge, R., Wernicke, A. G. Advances in radiotherapy for glioblastoma. *Frontiers in Neurology*. **8**, 748 (2018).
8. Ling, C. C. et al. Towards multidimensional radiotherapy (MD-CRT): Biological imaging and biological conformality. *International Journal of Radiation Oncology, Biology, Physics*. **47** (3), 551–560 (2000).
9. Bentzen, S. M., Gregoire, V. Molecular imaging-based dose painting: a novel paradigm for radiation therapy prescription. *Seminars in Radiation Oncology*. **21** (2), 101–110 (2011).
10. Bentzen, S. M. Theragnostic imaging for radiation oncology: Dose-painting by numbers. *The Lancet. Oncology*. **6** (2), 112–117 (2005).
11. Wong, J. et al. High-resolution, small animal radiation research platform with X-ray tomographic guidance capabilities. *International Journal of Radiation Oncology, Biology, Physics*. **71** (5), 1591–1599 (2008).
12. Van Hoof, S. J., Granton, P. V., Verhaegen, F. Development and validation of a treatment planning system for small animal radiotherapy: SmART-Plan. *Radiotherapy and Oncology*. **109** (3), 361–366 (2013).
13. Verhaegen, F., Granton, P., Tryggestad, E. Small animal radiotherapy research platforms. *Physics in Medicine & Biology*. **56** (12), R55–R83 (2011).
14. Butterworth, K. T., Prise, K. M., Verhaegen, F. Small animal image-guided radiotherapy: Status, considerations and potential for translational impact. *The British Journal of Radiology*. **88** (1045), 20140634 (2015).

15. Nasr, A., Habash, A. Dosimetric analytic comparison of inverse and forward planned IMRT techniques in the treatment of head and neck cancer. *Journal of the Egyptian National Cancer Institute*. **26** (3), 119–125 (2014).
16. Matinfar, M., Iyer, S., Ford, E., Wong, J., Kazanzides, P. Image guided complex dose delivery for small animal radiotherapy. *IEEE International Symposium on Biomedical Imaging: From Nano to Macro*, 1243–1246 (2009).
17. Matinfar, M., Iordachita, I., Wong, J., Kazanzides, P. Robotic delivery of complex radiation volumes for small animal research. *IEEE International Conference on Robotics and Automation*. 2056–2061 (2010).
18. Balvert, M. et al. A framework for inverse planning of beam-on times for 3D small animal radiotherapy using interactive multi-objective optimisation. *Physics in Medicine & Biology*. **60** (14), 5681–5698 (2015).
19. Cho, N. B., Wong, J., Kazanzides, P. Dose Painting with a Variable Collimator for the Small Animal Radiation Research Platform (SARRP). *The Midas Journal*. 1–8 (2014).
20. Bolcaen, J. et al. MRI-guided 3D conformal arc micro-irradiation of a F98 glioblastoma rat model using the Small Animal Radiation Research Platform (SARRP). *Journal of Neuro-oncology*. **120** (2), 257–266 (2014).
21. Bolcaen, J., Descamps, B., Boterberg, T., Vanhove, C., Goethals, I. PET and MRI guided irradiation of a glioblastoma rat model using a micro-irradiator. *Journal of Visualized Experiments: JoVE*. (130), 56601 (2017).
22. Verhoeven, J. et al. Technical feasibility of [ $^{18}\text{F}$ ]FET and [ $^{18}\text{F}$ ]FAZA PET guided radiotherapy in a F98 glioblastoma rat model. *Radiation Oncology*. **14** (1), 89 (2019).
23. Hutterer, M. et al. FET PET: a valuable diagnostic tool in neuro-oncology, but not all that glitters is glioma. *Neuro-oncology*. **15** (3), 341–351 (2013).
24. Stockhammer, F., Plotkin, M., Amthauer, H., Landeghem, F. K. H., Woiciechowsky, C. Correlation of F-18-fluoro-ethyl-tyrosin uptake with vascular and cell density in non-contrast-enhancing gliomas. *Journal of Neuro-oncology*. **88** (2), 205–210 (2008).
25. Rorden, C., Karnath, H. O., Bonhilha, L. Mricron dicom to nifti converter. neuroimaging informatics tools and resources clearinghouse (nitrc). <https://www.nitrc.org/projects/mricron> (2015).
26. Ashburner, J. et al. *SPM12 Manual*. [https://www.fil.ion.ucl.ac.uk/spm/doc/spm12\\_manual.pdf](https://www.fil.ion.ucl.ac.uk/spm/doc/spm12_manual.pdf) (2014).
27. España, S., Marcinkowski, R., Keereman, V., Vandenberghe, S., Van Holen, R. DigiPET: Sub-millimeter spatial resolution small-animal PET imaging using thin monolithic scintillators. *Physics in Medicine & Biology*. **59** (13), 3405–3420 (2014).

**TITLE:**

Positron Emission Tomography-based Dose Painting Radiation Therapy In A Glioblastoma Rat Model Using The Small Animal Radiation Research Platform

**AUTHORS AND AFFILIATIONS:**

Sam Donche<sup>1</sup>, Jeroen Verhoeven<sup>1</sup>, Benedicte Descamps<sup>2</sup>, Charlotte Bouckaert<sup>3</sup>, Robrecht Raedt<sup>3</sup>, Christian Vanhove<sup>2</sup>, Ingeborg Goethals<sup>1</sup>

<sup>1</sup>Department of Diagnostic Sciences, Ghent University, Ghent, Belgium

<sup>2</sup>Department of Electronics and Information Systems, Ghent University, Ghent, Belgium

<sup>3</sup>Department of Head and Skin, Ghent University, Ghent, Belgium

**Email addresses of co-authors:**

Sam Donche	(Sam.Donche@UGent.be)
Benedicte Descamps	(Benedicte.Descamps@UGent.be)
Charlotte Bouckaert	(Charlotte.Bouckaert@UGent.be)
Robrecht Raedt	(Robrecht.raedt@UGent.be)
Christian Vanhove	(Christian.Vanhove@UGent.be)

**Corresponding authors:**

Jeroen Verhoeven	(Jeroen.Verhoeven@UGent.be)
Ingeborg Goethals	(Ingeborg.Goethals@UGent.be)

**KEYWORDS:**Cancer research, small animal irradiation, glioblastoma, magnetic resonance imaging, positron emission tomography, image-guided irradiation, dose-painting-by-numbers, inverse planning

**SUMMARY:**

Here we present a protocol to perform preclinical positron emission tomography-based radiotherapy in a rat glioblastoma model using algorithms developed in-house to optimize the accuracy and efficiency.

**ABSTRACT:**

A rat glioblastoma model to mimic chemo-radiation treatment of human glioblastoma in the clinic was previously established. Similar to the clinical treatment, computed tomography (CT) and magnetic resonance imaging (MRI) were combined during the treatment-planning process. Positron emission tomography (PET) imaging was subsequently added to implement sub-volume boosting using a micro-irradiation system. However, combining three imaging modalities (CT, MRI, and PET) using a micro-irradiation system proved to be labor-intensive because multimodal imaging, treatment planning, and dose delivery have to be completed sequentially in the preclinical setting. This also results in a workflow that is more prone to human error. Therefore, a user-friendly algorithm to further optimize preclinical multimodal imaging-based radiation treatment planning was implemented. This software tool was used to evaluate the accuracy and efficiency of dose painting radiation therapy with micro-irradiation by using an *in silico* study design. The new methodology for dose painting radiation therapy is superior to the previously described method in terms of accuracy, time efficiency, and intra- and inter-user variability. It is



also an important step towards the implementation of inverse treatment planning on micro-irradiators, where forward planning is still commonly used, in contrast to clinical systems.

## INTRODUCTION:

Glioblastoma (GB) is a malignant and very aggressive primary brain tumor. GB is a solid heterogeneous tumor typically characterized by infiltrative boundaries, nuclear atypia, and necrosis<sup>1</sup>. The presence of the blood-brain-barrier and the brain's status as an immune-privileged site makes the discovery of novel targets for chemo- and immunotherapy a daunting task<sup>2-4</sup>. It is noteworthy that the treatment of GB patients has barely changed since the introduction, in 2005, of the Stupp protocol that combines external beam radiation therapy (RT) with concomitant temozolomide, usually followed by adjuvant temozolomide<sup>5</sup>. Typically, the Stupp protocol is preceded by maximal surgical resection. Therefore, alternative treatment approaches are of pivotal importance.

Current radiation therapy for glioblastoma patients delivers a uniform radiation dose to the defined tumor volume. In radiation oncology, there is an important dose-response correlation for glioblastoma with increasing dose, which seems to cap around 60 Gy, due to increased toxicity to the normal brain<sup>6,7</sup>. However, tumors can be very (radiobiologically) heterogeneous, with gradients of oxygen level and/or large differences in cellular density. Metabolic imaging techniques, such as PET, can visualize these biological features and can be utilized to customize the dose prescription. This approach is known as dose painting RT. This term was introduced by Ling et al. in 2000. The authors defined dose painting RT as producing "exquisitely conformal dose distributions within the constraints of radiation propagation and scatter"<sup>8</sup>.

There are two types of dose painting RT, dose painting by contours (DPBC), by which a dose is prescribed to a set of nested sub-volumes, and dose painting by numbers (DPBN), whereby a dose is prescribed at the voxel level. The dose distribution for DPBN RT can be extracted from functional images. The dose in each voxel is determined by the intensity  $I$  of the corresponding voxel in the image, with a lower and upper limit, to make sure that, on the one hand, a sufficient dose is delivered to every part of the tumor. On the other hand, doses do not exceed an upper limit to protect organs at risk and avoid toxicity. The most straightforward method is a linear interpolation (see **Eq. 1**) between minimum dose  $D_{min}$  and maximum dose  $D_{max}$ , proportionally varying between minimum intensity  $I_{min}$  and maximum intensity  $I_{max}$  within the target volume<sup>9,10</sup>:

$$D_I = D_{low} + \frac{I - I_{low}}{I_{high} - I_{low}} (D_{high} - D_{low}) \quad \text{Eq. 1}$$

Because there is some skepticism about the quality assurance of DPBN RT, the deposition of the dose should be verified through preclinical and clinical research<sup>10</sup>. However, only limited data can be acquired from clinical trials, and it has been hypothesized that more insights can be obtained by downscaling to laboratory animals<sup>11,12</sup>. Hence, preclinical studies utilizing precision image-guided radiation research platforms that allow coupling with some very specific techniques, such as autoradiography, are suited for examining open issues and paving the way

towards personalized medicine and novel treatment strategies, such as dose painting RT<sup>13,14</sup>. However, the interpretation of preclinical data must be performed with caution, and drawbacks of these preclinical setups have to be considered<sup>14</sup>.

Micro-irradiation systems, such as the Small Animal Radiation Research Platform (SARRP), are equipped with similar technologies as their clinical counterpart. They include on-board cone-beam CT (CBCT) imaging, a preclinical treatment-planning system (PCTPS), and provide sub-millimeter precision. Clinical dose calculations are performed by inverse treatment planning, whereby one initiates from the desired dose distribution to determine the beams via an iterative algorithm. Preclinical irradiators often use forward planning. In forward planning, the required amount and angle of the beams are selected, and the PCTPS then calculates the dose distribution. The optimization of the plans is performed by manual iteration, which is labor-intensive<sup>15</sup>.

After 2009, novel developments have made the implementation of inverse planning on these research platforms possible<sup>16–18</sup>. To increase the similarity with the clinical method, a motorized variable rectangular collimator (MVC) was developed as a preclinical counterpart of the multi-leaf collimator. A two-dimensional dose painting method utilizing a variable collimator was published by Cho et al.<sup>19</sup>. This research group implemented a three-dimensional (3D) inverse treatment-planning protocol on a micro-irradiator and determined minimum and maximum doses for the target volume and a maximum dose for the organs at risk. These techniques have mainly been evaluated *in silico*, and their preclinical applications need to be explored.

This paper presents an *in silico* study to compare two methodologies for [<sup>18</sup>F]-fluoro-ethyl-L-tyrosine ([<sup>18</sup>F]FET) PET-based dose painting in a GB rat model<sup>20–22</sup> using a small animal radiation research platform. These two methodologies are (1) sub-volume boosting using predefined beam sizes and (2) dose painting using a motorized variable collimator where jaw dimensions are modified based on the PET tracer uptake in the tumor volume. [<sup>18</sup>F]FET is a PET tracer often used in neuro-oncology because of its ability to detect brain tumors<sup>23</sup>. [<sup>18</sup>F]FET is an artificial amino acid that is internalized into tumoral cells but not incorporated into cell proteins. [<sup>18</sup>F]FET uptake corresponds with cell proliferation rate, tumor cell density, and angiogenesis<sup>24</sup>. As this is the most commonly used oncologic brain PET tracer in these authors' institute, this radiotracer was chosen to evaluate the new workflow.

## PROTOCOL:

The study was approved by the local ethics committee for animal experiments (ECD 18/21).

### 1. F98 GB rat cell model

1.1. Culture the F98 GB cells in a monolayer using Dulbecco's Modified Eagle Medium, supplemented with 10% calf serum, 1% penicillin, 1% streptomycin, and 1% L-glutamine, and place them in a CO<sub>2</sub> incubator (5% CO<sub>2</sub> and 37 °C).

1.2. Inoculate the glioma cells into the brain of female Fischer F344 rats (body weight 170 g).

NOTE: Use sterile instruments and wear sterile gloves at all times.

1.2.1. Anesthetize the rats through the inhalation of isoflurane (5% induction, 2% maintenance) mixed with oxygen (0.3 mL/min) through a nose cone. Confirm the anesthetization by the absence of withdrawal reflex of the limb, and immobilize the rats in a stereotactic device using fixation points for the nose and ears. Apply a carbomer eye gel to prevent dry eyes under anesthesia. Maintain the body temperature by a thermoregulated heating pad and rectal probe at 37 °C.

1.2.2. Shave the rat from the eye level to the back of the skull, and disinfect the skin with isobetadine. Inject xylocaine (with adrenaline 1:200000, 0.1 mL) subcutaneously for local anesthesia.

1.2.3. Expose the skull through a midline scalp incision and make a small hole with a drill tool 3 mm posterior and 3 mm lateral to the bregma in the right hemisphere.

1.2.4. Insert a stereotactically guided insulin needle (29 G) and inject 5 µL of cell suspension (20,000 F98 GB cells) 3 mm deep using a microsyringe pump controller. Leave the needle in place for 5 min, giving the cell suspension time to diffuse into the tissue.

1.2.5. Withdraw the syringe slowly and close the hole in the skull with bone wax. Suture the skin (polyamide 6, thickness 4-0) and inject meloxicam subcutaneously (1 mg/kg, 2 mg/mL). Apply xylocaine gel.

1.2.6. Stabilize the body temperature of the animal post-surgery using a red lamp. Monitor the awakening of the rat until it has regained sufficient consciousness. Do not return the animal to the company of other animals until fully recovered. House all animals under environmentally controlled conditions (12 h light/dark cycle, 20–24 °C, and 40–70% relative humidity) with food and water *ad libitum*.

1.2.7. Be sure to monitor the animals daily and maintain a daily health status log by checking their body weight, food, water intake, and their activity and behavior. Use a lethal dose of pentobarbital sodium to euthanize the animals (160 mg/kg) if a decline of 20% body weight is observed or when the normal behavior severely deteriorates (e.g., lack of grooming).

## 2. Confirmation of tumor growth

2.1. Evaluate tumor growth 8 days post-inoculation. Anesthetize the rats through the inhalation of isoflurane (5% induction, 2% maintenance) mixed with oxygen (0.3 mL/min) through a nose cone. Confirm the anesthetization by the absence of withdrawal reflex of the limb.

2.2. Inject a gadolinium-containing contrast agent (0.4 mL/kg) through an intravenously placed tubing in the lateral tail vein. Cover the animal with a heated blanket and place them in the MRI bed. Apply a carbomer eye gel to prevent dry eyes under anesthesia. Place the MRI bed

in the holder with a Tx/Rx Rat brain volume coil.

2.3. Perform a localizer scan followed by a T<sub>2</sub>-weighted spin-echo scan to assess tumor growth. Use these T<sub>2</sub>-MRI sequence settings: repetition time (TR)/echo time (TE) 3661/37.1 ms, 109 μm isotropic in-plane resolution, slice thickness 600 μm, 4 averages, 30 slices, total acquisition time (TA) 9 min 45 s.

2.4. If a tumor is confirmed on the T<sub>2</sub>-weighted acquisition, perform a T<sub>1</sub>-weighted contrast-enhanced spin echo scan. Use these T<sub>1</sub>-MRI sequence settings: TR/TE 1539/9.7 ms, 0.117 mm isotropic in-plane resolution, slice thickness 600 μm, 3 averages, 30 slices, TA 4 min 15 s.

2.5. After the MRI, continuously supervise the animal until it regains full consciousness.

2.6. When the tumor reaches a diameter of 7 to 8 mm, usually observed 12 days after inoculation, select the animal for therapy.

### 3. Multimodality imaging of target volume selection

NOTE: PET/MRI-guided irradiation requires the sequential acquisition of a multimodal dataset. After intravenous administration of the radiotracer, PET imaging is started, followed by contrast-enhanced T<sub>1</sub>-weighted MRI and finally a treatment-planning CT.

3.1. Anesthetize the animal with isoflurane (5% induction, 2% maintenance) mixed with oxygen (0.3 L/min) using a nose cone. Confirm anesthetization when the rats do not exhibit any withdrawal reflex of the limb. Apply carbomer eye gel to prevent dry eyes under anesthesia.

3.2. Insert the tubing intravenously in the lateral tail vein, enabling the injection of 10–12 MBq of PET radioactive tracer dissolved in 200 μL of saline. Inject [<sup>18</sup>F]-FET, 1 h before PET acquisition. Let the animal regain consciousness while the tracer is distributed through the body.

3.3. Anesthetize the animal again, as described in step 3.1. Place the animal on a multimodality bed (here, made in-house) and secure it using hook-and-loop fasteners, maintaining a fixed position during the imaging and micro-irradiation. Fix a capillary filled with the MRI/PET agent (see the **Table of Materials**) for easier co-registration. Wrap the animal in bubble wrap to preserve its body temperature during the multimodality imaging and therapy.

3.4. Perform a PET scan 1 h after the injection of the PET tracer. Reconstruct the PET scan into a 3D volume (192 x 192 x 384 matrix) with 0.4 mm voxel size by applying a Maximum-Likelihood Expectation-Maximization (MLEM)-algorithm using 30 iterations.

NOTE: A dedicated PET scanner for laboratory animal imaging was used with an axial field of view of 130 mm and a bore diameter of 72 mm. This system provides sub-mm (0.85 mm) spatial resolution.

3.5. Inject an MRI contrast agent (0.4 mL/kg) intravenously into the tail vein. Place the rat, still fixed on the multimodality bed, in the animal holder of the MRI scanner (**Table of Materials**). Perform a localizer scan followed by a contrast-enhanced T<sub>1</sub>-weighted spin-echo sequence, analogous to step 2.4.

3.6. Place the animal, still fixed on the multimodality bed, on a plastic holder secured onto the four-axis robotic positioning table on the micro-irradiator. Perform a high-resolution treatment-planning cone-beam CT using a tube voltage of 70 kV, a tube current of 0.4 mA, a 1 mm aluminum filter, and a 20 x 20 cm (1024 x 1024 pixel) amorphous Si flat panel detector. Acquire a total of 360 projections over 360°. Reconstruct the CT images with an isotropic voxel size of 0.275 mm (411 x 411 x 251 matrix).

#### 4. Image co-registration

NOTE: The co-registration is performed with a semi-automatic MATLAB code developed in-house. The code can be found on Github at <https://github.com/sdonche/DosePainting>. The different steps are described below.

4.1. Place the three image modalities ([<sup>18</sup>F]FET PET, contrast-enhanced T<sub>1</sub>-weighted MRI, and cone-beam CT) into one folder. Convert DICOM images to the **NIfTI format** using the **dcm2niix** function from the **mricon image viewer**<sup>24</sup>.

4.2. Import the converted images into MATLAB and filter the PET image with a Gaussian filter using a **Full-Width Half-Max (FWHM) of 1 mm**.

4.3. Reorient the images so that the cartesian axes from all imaging modalities correspond with each other.

NOTE: For this setup, the CT image was flipped around the Y-axis; the MRI was flipped around the X-axis, and the PET was flipped around the Y-axis.

4.4. Crop the PET image to simplify automatic co-registration.

NOTE: For this setup, 40 pixels were set to zero from both sides of the X-axis (left and right of the animal); on the dorsal and ventral side of the animal (Y-axis), 60 and 40 pixels were set to zero, respectively; along the longitudinal axis (or Z-axis), 170 and 30 pixels are set to zero for inferior and superior side, respectively.

4.5. Move the image centers close to each other to simplify automatic co-registration.

4.6. Perform the actual rigid-body co-registration using Statistical Parametric Mapping (SPM) in MATLAB<sup>26</sup>. Use the following registration parameters (others on default): objective function: mutual information; separation: [4 1 0.2]; tolerances: [0.02 0.02 0.02 0.001 0.001 0.001 0.01 0.01 0.01 0.001 0.001 0.001]; histogram smoothing: [1 1]; interpolation: trilinear.

## 5. Radiation treatment planning

NOTE: A MATLAB app and multiple MATLAB scripts were written for the radiation treatment planning. The code can be found on Github at <https://github.com/sdonche/DosePainting>. The different steps are explained below.

### 5.1. Method 1

5.1.1. Load the three different imaging modalities into the MATLAB app. Place a generous bounding box around the contrast enhancement on the T<sub>1</sub>-weighted MRI scan (**Figure 1**). Determine the contrast-enhanced volume using a threshold (**Figure 2**). If multiple regions have been selected, select only the largest volume, the center of which is considered as the first isocenter to deliver a prescribed dose for RT (**Figure 3**).

5.1.2. Expand the previously determined MRI contrast enhancement by 10 pixels in each direction. If multiple regions are detected, retain only the largest PET volume, the center of which is considered the second isocenter to deliver a prescribed dose for RT.

NOTE: In this PET volume, the PET boost volume is defined by the pixels with a higher signal intensity than  $0.90 \times$  maximal signal intensity (in the bounding box) in this volume.

5.1.3. Use the following irradiation settings for the calculated isocenters (**Figure 4** and **Table 1**).

5.1.3.1. For the first isocenter (MRI), give a prescribed dose of 2000 cGy using 3 non-coplanar arcs at couch positions 0°, -45°, and -90° with a gantry rotation of 120°, 120°, and 60°, respectively. Use a fixed collimator size of 10 x 10 mm, but use an appropriate collimator (e.g., a 5 x 5 mm collimator) when smaller tumor sizes need to be irradiated. Be careful in considering the animal's welfare when the tumor volumes are larger than 10 mm.

5.1.3.2. For the second isocenter (PET), give a prescribed dose of 800 cGy using 3 non-coplanar arcs at couch positions 0°, -45°, and -90° with a gantry rotation of 120°, 120°, and 60°, respectively. Use a fixed collimator size of 3 x 3 mm.

5.1.4. Calculate the dose distribution within the animal and the beam delivery parameters.

### 5.2. Method 2

5.2.1. Load the three different imaging modalities into the MATLAB app. Place a generous bounding box around the contrast-enhancement on the [<sup>18</sup>F]FET PET image, analogous to step 5.1.1.

5.2.2. Determine the volumes defined by the pixels with a signal intensity higher than  $A \times$  maximal signal intensity (in the aforementioned bounding box), with A equal to 0.50, 0.60, 0.70,

0.80, and 0.90. Name these volumes V50, V60, V70, V80, and V90, respectively.

5.2.3. Determine the isocenters and the jaw dimensions for each beam required to guide the motorized variable collimator using the MATLAB script (see **Figure 5**).

5.3.3. Use the following settings for the calculated isocenters and jaw dimensions:

5.3.3.1. For V50, give a prescribed dose of 2000 cGy distributed over 16 beams (each 125 cGy; couch and gantry positions in **Table 2**). Use the calculated jaw dimensions for the MVC.

NOTE: Here, an additional margin of 1 mm has been included to account for microscopic tumor infiltration.

5.3.3.2. For V60–V90, give a prescribed dose of 800 cGy distributed over 40 beams (each 20 cGy; couch and gantry positions in **Table 2**). Use the calculated jaw dimensions for the MVC.

5.3.4. Calculate the dose distribution within the animal and the beam delivery parameters.

## 6. Plan evaluation

NOTE: To compare the two methods, calculate the dose-volume histograms (DVH) and Q-volume histogram (QVH) in the V50 PET volume. Here, a MATLAB script, developed in-house, was used. The code can be found on Github at <https://github.com/sdonche/DosePainting>.

### 6.1. Dose-volume histogram

6.1.1. Generate DVH from the dose distribution that was obtained from the SARRP.

6.1.2. Determine the maximum, mean, and minimum doses from the DVH by calculating the  $D_{10}$ ,  $D_{50}$ , and  $D_{90}$ , where  $D_x$  stands for the dose received by  $x\%$  of the volume.

### 6.2. Q-volume histogram

6.2.1. Calculate an ideal dose for every pixel using **Eq. 1**, which is a linear interpolation between the minimum and maximum doses, proportionally varying between the minimum PET intensity and maximum PET intensity within the target volume to give an ideal dose map.

6.2.2. Calculate the Q-value  $Q_p$  for every pixel using the following equation (**Eq. 2**):

$$Q_p = \frac{D_p}{D_i} \quad \text{Eq. 2}$$

With  $D_p$  being the dose obtained by planning and  $D_i$ , the dose objective for planning.

6.2.3. Generate QVH from the obtained Q-values.

6.2.4. Calculate the quality factor (Q-factor,  $Q_F$ ) to evaluate the difference between the planned and intended doses using Eq. 3:

$$Q_F = \frac{1}{n} \sum_{p=1}^{p=n} |Q_p - 1|$$

Eq.  
3

## REPRESENTATIVE RESULTS:

The feasibility of PET- and MRI-guided irradiation in a glioblastoma rat model using the SARRP to mimic the human treatment strategy has been previously described<sup>20–22</sup>. While the animal was fixed on a multimodality bed made in-house, it was possible to create an acceptable radiation treatment plan combining three imaging modalities: PET, MRI, and CT. In these methods, an external software package (see the **Table of Materials**) was used to co-register the images using rigid-body transformations manually. The contrast-enhanced T<sub>1</sub>-weighted MRI and PET images were visually assessed from which the isocenters were manually selected. However, this methodology proved to be labor-intensive and certainly has an impact on the animals as they have to stay under general anesthesia during the multimodality imaging and the creation of a treatment plan. Therefore, the new methodology aims to automate specific steps in this process to reduce the overall variance and time required to create a radiation treatment plan.

In this paper, two methodologies are compared. Method 1 is very similar to the previously published methodology<sup>20–22</sup> with a few adjustments (**Table 1**). However, in contrast to the previously published methodology, most of the process is automated using a MATLAB code developed in-house. Method 2 is a more sophisticated method in which a series of isocenters and jaw dimensions for the MVC will be determined based on the [<sup>18</sup>F]FET PET uptake (**Figure 5**). The isocontours for V50, V60, V70, V80, and V90 are shown in **Figure 6**.

Both methods were applied to three different cases (**Figure 7**). These cases can be divided into two different types: [<sup>18</sup>F]FET PET uptake in the infiltrative tumor front and the presence of tumor necrosis and [<sup>18</sup>F]FET PET uptake indicating no tumor necrosis. Case 1 can be described as a spherical homogeneous PET uptake, while Cases 2 and 3 have a ring-shaped uptake where the reduced PET-uptake is most likely necrotic tissue. Case 3 also shows an additional region growing out towards the dorsal region.

After calculating the setup parameters for both methods, the dose distributions for each case (**Figure 8**) were determined using the SARRP's PCTPS. The DVHs (**Figure 9**) can be obtained from the dose distributions in the volumes defined by the pixels with signal intensity higher than 0.50 × maximal PET signal intensity (in the bounding box). One can observe that the DVHs for Method 2 are systematically closer to the ideal dose distribution than those for Method 1. A substantial tumor volume receives insufficient irradiation in Cases 2 and 3 when treated with Method 1. **Table 3** confirms these conclusions: the D<sub>90</sub> and D<sub>50</sub> values are considerably lower for Method 1 than for Method 2. The QVHs (**Figure 10**) can also be obtained from these dose distributions.



Ideally, these curves make a sharp drop at a Q-value equal to one. Method 2 always results in dose distributions that are closer to the dose objective. **Table 4** also demonstrates superior overall Q-factors for Method 2. The minimal dose ( $D_{90}$ ) of 2000 cGy has been achieved for all cases with Method 2, while it was not achieved with Method 1 in 2 cases. This means that the tumor volume received insufficient irradiation using Method 1.

#### FIGURE AND TABLE LEGENDS:

**Figure 1: Bounding box placement.** The  $T_1$ -weighted contrast enhancement is visible in the F98 GB rat model, and a generous bounding box is placed around the tumor using the MATLAB code developed in-house.

**Figure 2:  $T_1$ -weighted contrast-enhancing tumor delineation: step 1.** The tumor volume is delineated on the contrast-enhanced  $T_1$ -weighted MRI using thresholding. Abbreviation: MRI = magnetic resonance imaging.

**Figure 3:  $T_1$ -weighted contrast-enhancing tumor delineation: step 2.** If multiple volumes are detected during the thresholding step, the largest volume is retained for further processing.

**Figure 4: Isocenter calculation for Method 1.** Contrast-enhanced  $T_1$ -weighted MRI, CT, and PET images are depicted. The blue and red circles represent the MRI- and PET-based isocenters, respectively. Abbreviations: MRI = magnetic resonance imaging; CT = computed tomography; PET = positron emission tomography.

**Figure 5: Explanation of jaw setup calculation.** Step 1: the tumor volume is determined (blue dots, top image). Step 2: a plane (black grid) is created perpendicular to the incident beam (magenta line, top image) at specific couch and gantry positions. Step 3: the tumor voxels (blue dots, top image) are perpendicularly projected onto the aforementioned plane, resulting in a set of projected voxels (red dots). Step 4: determine the isocenter and jaw dimensions (green lines, bottom image) so that all the projected voxels are included within the rectangular beam defined by the two symmetrical jaws of the variable collimator (bottom image). These figures were generated in MATLAB.

**Figure 6: Tumor isocontours.** Transaxial, coronal, and sagittal slices through the brain tumor with tumor volumes V50, V60, V70, V80, and V90 determined by the isocontours corresponding to 50%, 60%, 70%, 80%, and 90% of the maximum tumor uptake in the PET images. Abbreviations: TV = transaxial; COR = coronal; SAG = sagittal; PET = positron emission tomography.

**Figure 7: [ $^{18}\text{F}$ ]FET PET imaging for the three cases.** The sagittal, transverse, and frontal views are displayed for all three cases.

**Figure 8: Dose distributions for both methods.** Sagittal, transverse, and frontal views for all three cases are displayed for both Method 1 and Method 2. The dose distribution is shown together with the cone-beam CT imaging from the SARRP. Abbreviations: CT = computed tomography;

SARRP = small animal radiation research platform.

**Figure 9: DVH curves for all cases.** DVH curves (in cGy) are shown for Method 1, Method 2, and the Ideal Dose Map. Abbreviation: DVH = dose-volume histogram.

**Figure 10: Q-volume histogram for all cases.** QVH curves are shown for Method 1, Method 2, and the Ideal Dose Map. Ideally, the calculated QVH must have a sharp drop at Q-value = 1 (Ideal dose map, blue line). Abbreviation: QVH = Q-volume histogram.

**Table 1: Method comparison.** This table further clarifies Method 1, Method 2, and the Previous Method (referring to the method that has already been published)<sup>20–22</sup>. Methods 1 and 2 utilize a preclinical PET scanner<sup>27</sup> with sub-millimeter spatial resolution, making it possible to visualize the tumor heterogeneity more clearly. At couch position -90°, it is only possible to use 60° out of 120° to avoid collision with the animal. Despite this drawback, this couch position has easier access to the tumor because it is situated in the right hemisphere. The other couch positions can make the full 120° rotations. Abbreviations: CE T<sub>1</sub> = contrast-enhanced T<sub>1</sub>-weighted; MVC = motorized variable collimator; PET = positron emission tomography.

**Table 2: Beam setup for Method 2.** The gantry and couch positions of all the different beams are displayed. V50 uses all configurations, whereas V60–V90 only use the configurations shown in bold.

**Table 1: DVH values.** D<sub>10</sub>, D<sub>50</sub>, and D<sub>90</sub> were calculated as substitutes for maximum, mean, and minimal doses, respectively. D<sub>x</sub> stands for the dose received by x% of the volume. Abbreviation: DVH = dose-volume histogram.

**Table 2: Q-factors.** The table displays the overall Q-factors for Method 1 and Method 2 for each case. The Q-factor will be zero if the delivered dose and prescribed dose are equal.

## DISCUSSION:

A rat GB model to mimic the chemo-radiation treatment in the clinic for glioblastoma patients was previously described<sup>20</sup>. Similar to the clinical method, CT and MRI were combined during the treatment-planning process to obtain more precise irradiation. A multimodality bed to minimize (head) movement was used when the animal was moved from one imaging system to another. Subsequently, PET imaging was added to the treatment-planning process, and PET-based sub-volume boosting could be successfully implemented<sup>21,22</sup>. The inclusion of a functional image modality, such as PET, in the treatment-planning process allows the visualization of the (biological) tumor heterogeneity. This facilitates the targeting of aggressive and/or radiation-resistant tumor regions. Although this method is feasible, it proved to be very labor-intensive because multimodal imaging, treatment planning, and dose delivery must be completed sequentially in a preclinical setting. Moreover, during this process, the animals have to stay under general anesthesia<sup>22</sup>. Therefore, it is essential to improve the efficiency of the preclinical treatment-planning process.

This paper presents a user-friendly semi-automatic algorithm to further optimize preclinical multimodal imaging-based radiation treatment planning. Co-registration between planning CT, MRI, and PET were automated, in combination with the detection of the target isocenters. Of note, the software tool should not be considered as a black box, and it is crucial to perform proper quality checks. The most critical step in this entire process is to evaluate the results of the automatic co-registration of planning CT, MRI, and PET that should be as accurate as possible. The output of the algorithm consists of the positions of the target isocenters and the jaw dimensions of the MVC for the different radiation beams. These values can be imported into the most recent version of the PCTPS.

This software tool was used to evaluate the accuracy and efficiency of PET-based dose painting on the micro-irradiator by using an *in silico* study design. The optimized treatment-planning process was superior to the previously described method<sup>21,22</sup> in terms of time efficiency, intra- and inter-user variability, and accuracy. While conventional preclinical treatment planning, including multimodal imaging, can require up to 180 min<sup>22</sup>, this time could be reduced to ~80 min with both the semi-automatic methods presented in this manuscript. Moreover, human errors are more likely in the conventional treatment-planning process during manual co-registration and visual determination of the isocenters, resulting in larger intra- and inter-user variability. The automatic co-registration and detection of the target isocenters by the algorithm will reduce these intra- and inter-user variabilities. In addition, the optimized and automated workflow provides more accurate irradiation of the tumor volume. This is illustrated by the lower Q-factors (**Table 4**), which assesses the difference between the dose calculated/delivered by the PCTPS and the prescribed dose.

It is also noteworthy that the use of an MVC results in a reduced dose to the surrounding normal brain tissue, compared to collimators with a fixed beam size. This is illustrated in **Figure 7** and is important to narrow the gap between clinical trials evaluating DPBN RT strategy (where multi-leaf collimators are used) and laboratory animal radiation research. However, we assume that dose delivery might be slightly slower when using an MVC to switch between beam positions and adjust the jaw dimensions for each individual beam. Finally, preclinical treatment planning is most often done by forward planning. The methodology described in this paper is a crucial step towards inverse planning, which is generally used in the clinic, and further narrows the gap between preclinical radiation research and the clinic.

This study also has some limitations. For the experiments described in this manuscript, the most commonly used amino acid PET tracer [<sup>18</sup>F]FET was used. When using other PET tracers to guide radiation treatment, the semi-automatic workflow should be properly examined because co-registration might be less accurate. Further, the impact of using a different voxel size for PET and/or MRI on treatment planning and dose delivery should be further investigated. In conclusion, the methodology described here to optimize the preclinical treatment-planning process has many advantages compared to the previously described method<sup>21,22</sup>. Using an *in silico* study design, it was proven that the novel workflow for preclinical multimodal treatment planning is more accurate in terms of dose delivery, more time-efficient, and shows less intra- and inter-user variability. These improvements are essential to narrow the gap between clinical

and preclinical radiation research and for the development of new therapeutics and/or radiation therapy procedures for glioblastoma.

#### **ACKNOWLEDGMENTS:**

The authors would like to thank Lux Luka Foundation for supporting this work.

#### **DISCLOSURES:**

The authors have no conflicts of interest to disclose.

#### **REFERENCES:**

1. Louis, D. N. et al. The 2016 World Health Organization classification of tumors of the central nervous system: a summary. *Acta Neuropathologica*. **131** (6), 803–820 (2016).
2. Wadajkar, A. S. et al. Tumor-targeted nanotherapeutics: Overcoming treatment barriers for glioblastoma. *Wiley Interdisciplinary Reviews. Nanomedicine & Nanobiotechnology*. **9** (4), 10.1002/wnan.1439 (2016).
3. Lim, M., Xia, Y., Bettegowda, C., Weller, M. Current state of immunotherapy for glioblastoma. *Nature Reviews. Clinical Oncology*. **15** (7), 422–422 (2018).
4. McGranahan, T., Li, G, Nagpal, S. History and current state of immunotherapy in glioma and brain metastasis. *Therapeutic Advances in Medical Oncology*. **9** (5), 347–368 (2017).
5. Stupp, R. et al. Radiotherapy plus concomitant and adjuvant temozolomide for glioblastoma. *The New England Journal of Medicine*. **352** (10), 987–996 (2005).
6. Von Neubeck, C., Seidlitz, A., Kitzler, H. H., Beuthien-Baumann, B., Krause, M. Glioblastoma multiforme: Emerging treatments and stratification markers beyond new drugs. *The British Journal of Radiology*. **88** (1053), 20150354 (2015).
7. Mann, J., Ramakrishna, R., Magge, R., Wernicke, A. G. Advances in radiotherapy for glioblastoma. *Frontiers in Neurology*. **8**, 748 (2018).
8. Ling, C. C. et al. Towards multidimensional radiotherapy (MD-CRT): Biological imaging and biological conformality. *International Journal of Radiation Oncology, Biology, Physics*. **47** (3), 551–560 (2000).
9. Bentzen, S. M., Gregoire, V. Molecular imaging-based dose painting: a novel paradigm for radiation therapy prescription. *Seminars in Radiation Oncology*. **21** (2), 101–110 (2011).
10. Bentzen, S. M. Theragnostic imaging for radiation oncology: Dose-painting by numbers. *The Lancet. Oncology*. **6** (2), 112–117 (2005).
11. Wong, J. et al. High-resolution, small animal radiation research platform with X-ray tomographic guidance capabilities. *International Journal of Radiation Oncology, Biology, Physics*. **71** (5), 1591–1599 (2008).
12. Van Hoof, S. J., Granton, P. V., Verhaegen, F. Development and validation of a treatment planning system for small animal radiotherapy: SmART-Plan. *Radiotherapy and Oncology*. **109** (3), 361–366 (2013).
13. Verhaegen, F., Granton, P., Tryggestad, E. Small animal radiotherapy research platforms. *Physics in Medicine & Biology*. **56** (12), R55–R83 (2011).
14. Butterworth, K. T., Prise, K. M., Verhaegen, F. Small animal image-guided radiotherapy: Status, considerations and potential for translational impact. *The British Journal of Radiology*. **88** (1045), 20140634 (2015).

15. Nasr, A., Habash, A. Dosimetric analytic comparison of inverse and forward planned IMRT techniques in the treatment of head and neck cancer. *Journal of the Egyptian National Cancer Institute*. **26** (3), 119–125 (2014).
16. Matinfar, M., Iyer, S., Ford, E., Wong, J., Kazanzides, P. Image guided complex dose delivery for small animal radiotherapy. *IEEE International Symposium on Biomedical Imaging: From Nano to Macro*, 1243–1246 (2009).
17. Matinfar, M., Iordachita, I., Wong, J., Kazanzides, P. Robotic delivery of complex radiation volumes for small animal research. *IEEE International Conference on Robotics and Automation*. 2056–2061 (2010).
18. Balvert, M. et al. A framework for inverse planning of beam-on times for 3D small animal radiotherapy using interactive multi-objective optimisation. *Physics in Medicine & Biology*. **60** (14), 5681–5698 (2015).
19. Cho, N. B., Wong, J., Kazanzides, P. Dose Painting with a Variable Collimator for the Small Animal Radiation Research Platform (SARRP). *The Midas Journal*. 1–8 (2014).
20. Bolcaen, J. et al. MRI-guided 3D conformal arc micro-irradiation of a F98 glioblastoma rat model using the Small Animal Radiation Research Platform (SARRP). *Journal of Neuro-oncology*. **120** (2), 257–266 (2014).
21. Bolcaen, J., Descamps, B., Boterberg, T., Vanhove, C., Goethals, I. PET and MRI guided irradiation of a glioblastoma rat model using a micro-irradiator. *Journal of Visualized Experiments: JoVE*. (130), 56601 (2017).
22. Verhoeven, J. et al. Technical feasibility of [ $^{18}\text{F}$ ]FET and [ $^{18}\text{F}$ ]FAZA PET guided radiotherapy in a F98 glioblastoma rat model. *Radiation Oncology*. **14** (1), 89 (2019).
23. Hutterer, M. et al. FET PET: a valuable diagnostic tool in neuro-oncology, but not all that glitters is glioma. *Neuro-oncology*. **15** (3), 341–351 (2013).
24. Stockhammer, F., Plotkin, M., Amthauer, H., Landeghem, F. K. H., Woiciechowsky, C. Correlation of F-18-fluoro-ethyl-tyrosin uptake with vascular and cell density in non-contrast-enhancing gliomas. *Journal of Neuro-oncology*. **88** (2), 205–210 (2008).
25. Rorden, C., Karnath, H. O., Bonhilha, L. Mricron dicom to nifti converter. neuroimaging informatics tools and resources clearinghouse (nitrc). <https://www.nitrc.org/projects/mricron> (2015).
26. Ashburner, J. et al. *SPM12 Manual*. [https://www.fil.ion.ucl.ac.uk/spm/doc/spm12\\_manual.pdf](https://www.fil.ion.ucl.ac.uk/spm/doc/spm12_manual.pdf) (2014).
27. España, S., Marcinkowski, R., Keereman, V., Vandenberghe, S., Van Holen, R. DigiPET: Sub-millimeter spatial resolution small-animal PET imaging using thin monolithic scintillators. *Physics in Medicine & Biology*. **59** (13), 3405–3420 (2014).

Figure 1

[Click here to access/download;Figure;Figure 1.jpg](#)

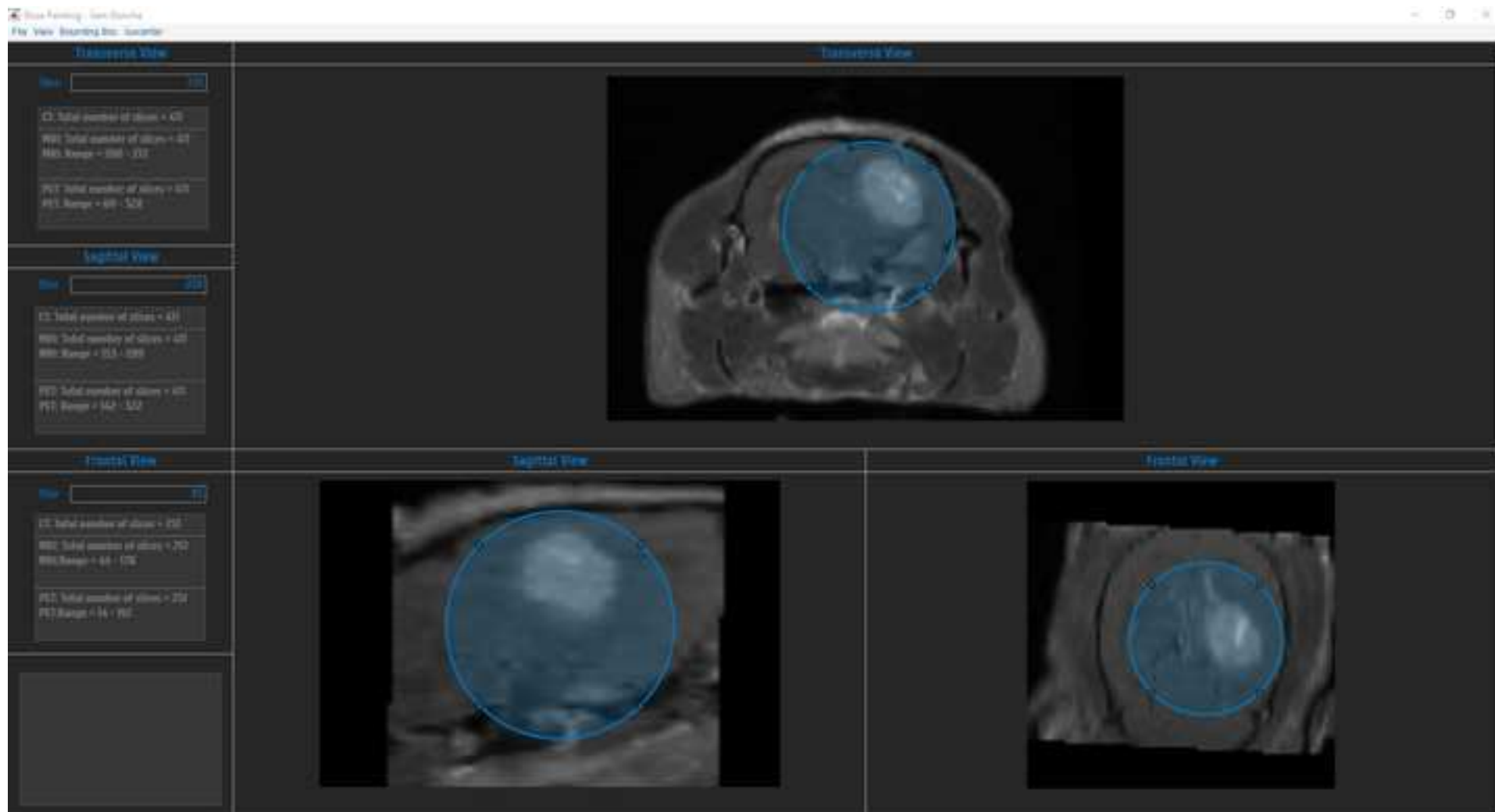


Figure 2

[Click here to access/download;Figure;Figure 2.jpg](#)

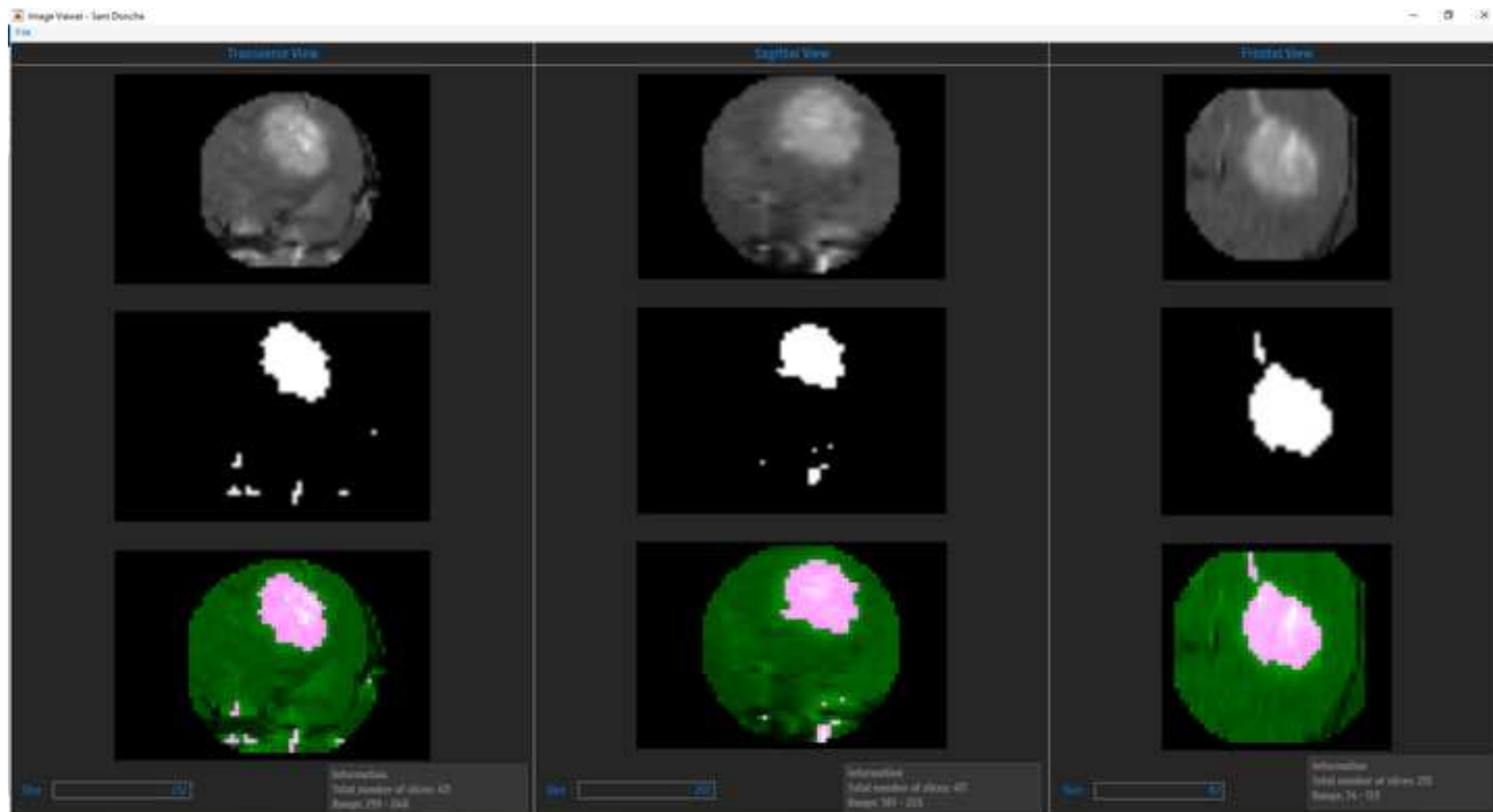


Figure 3

[Click here to access/download;Figure;Figure 3.jpg](#)

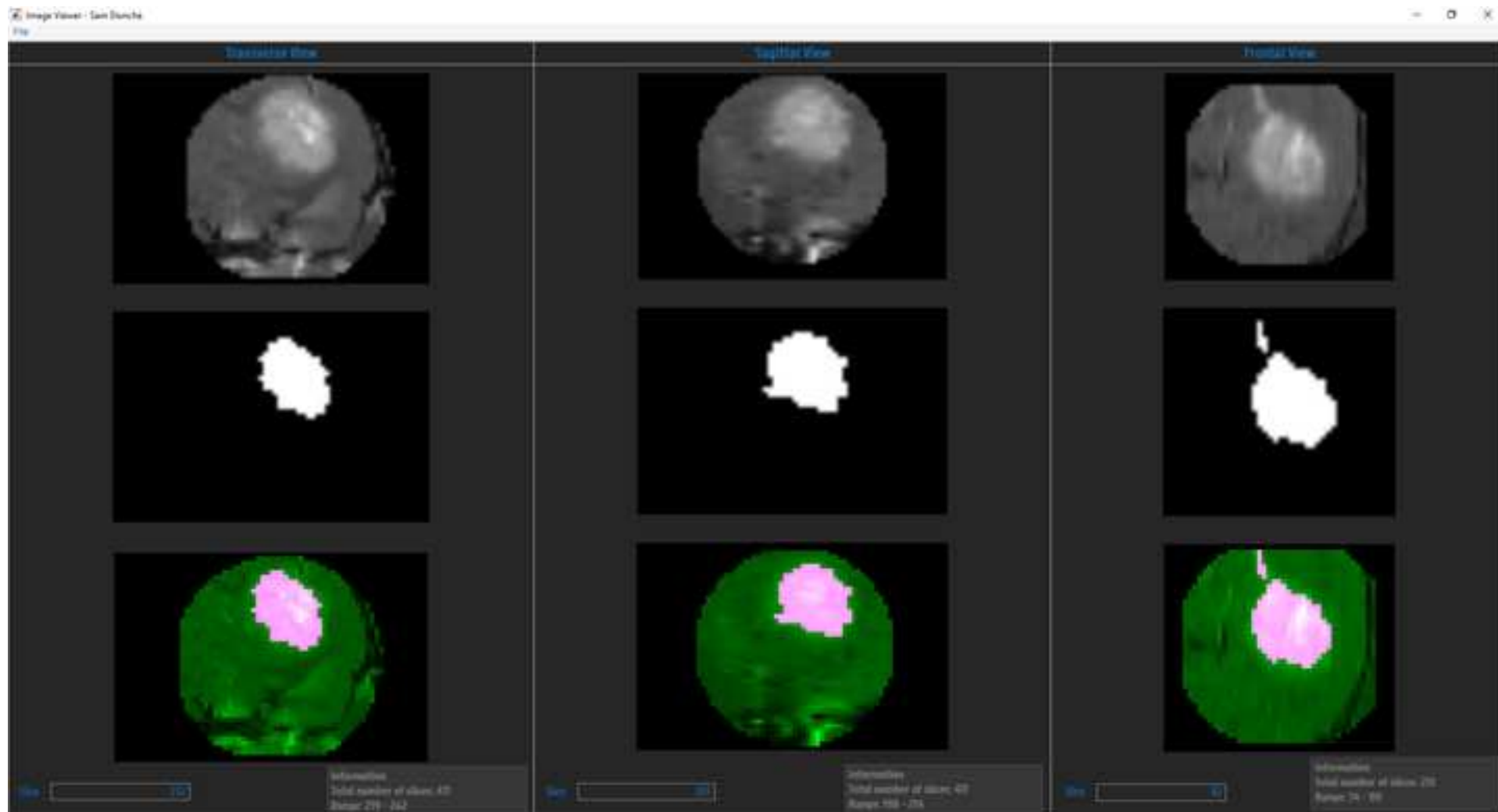




Figure 4

[Click here to access/download;Figure;Figure 4.jpg](#) 

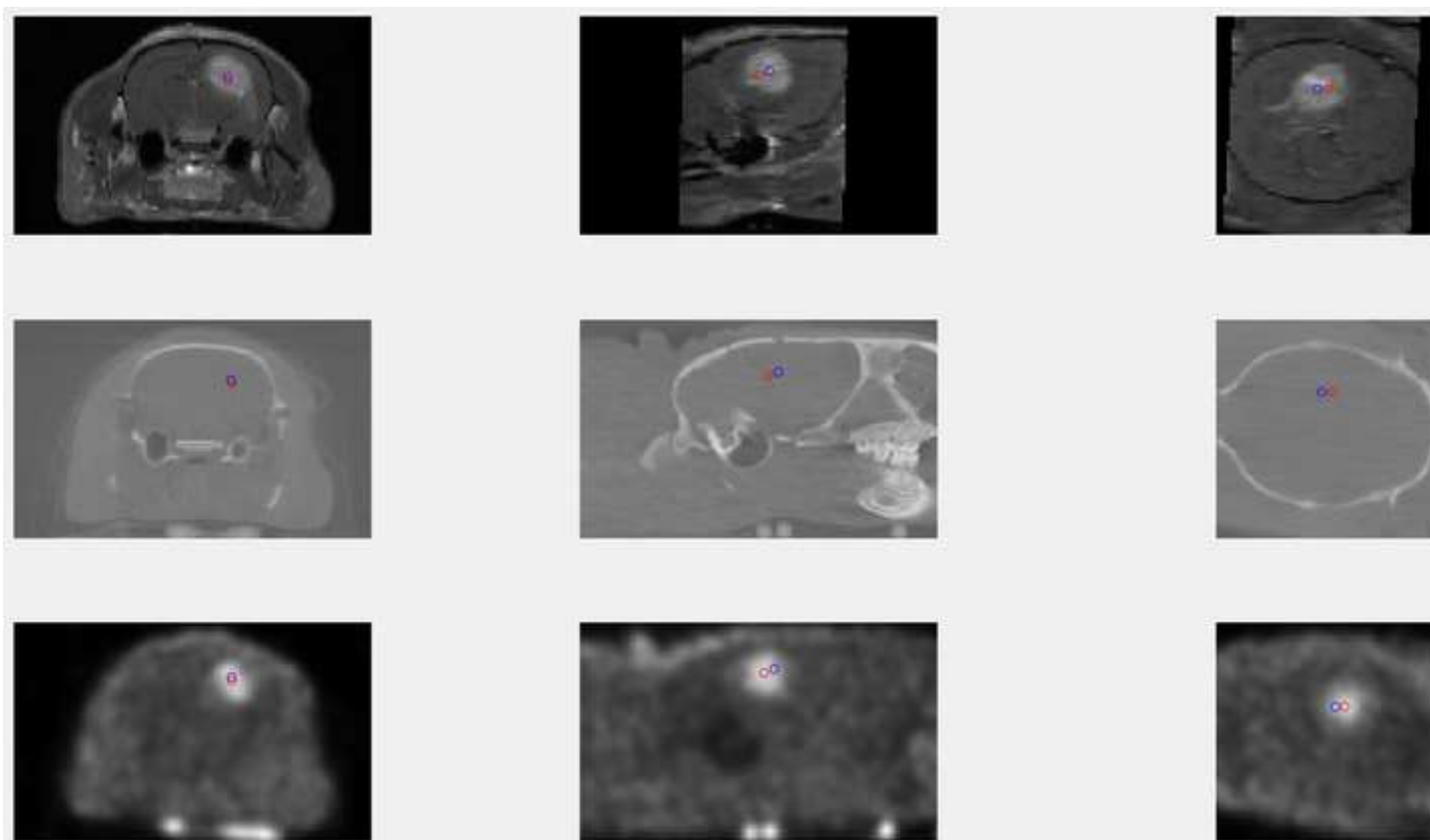
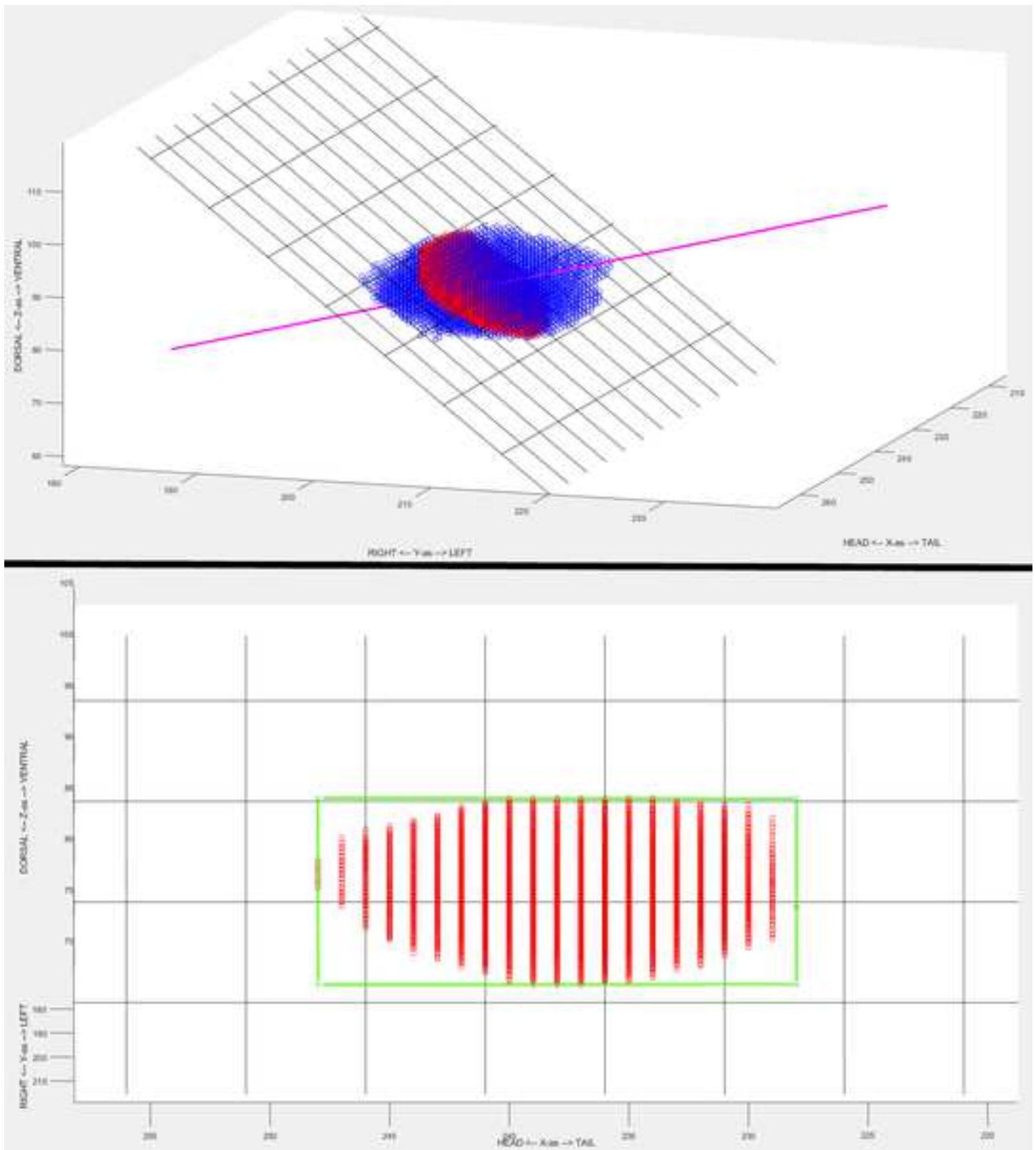


Figure 5

[Click here to access/download;Figure;Figure 5.jpg](#)



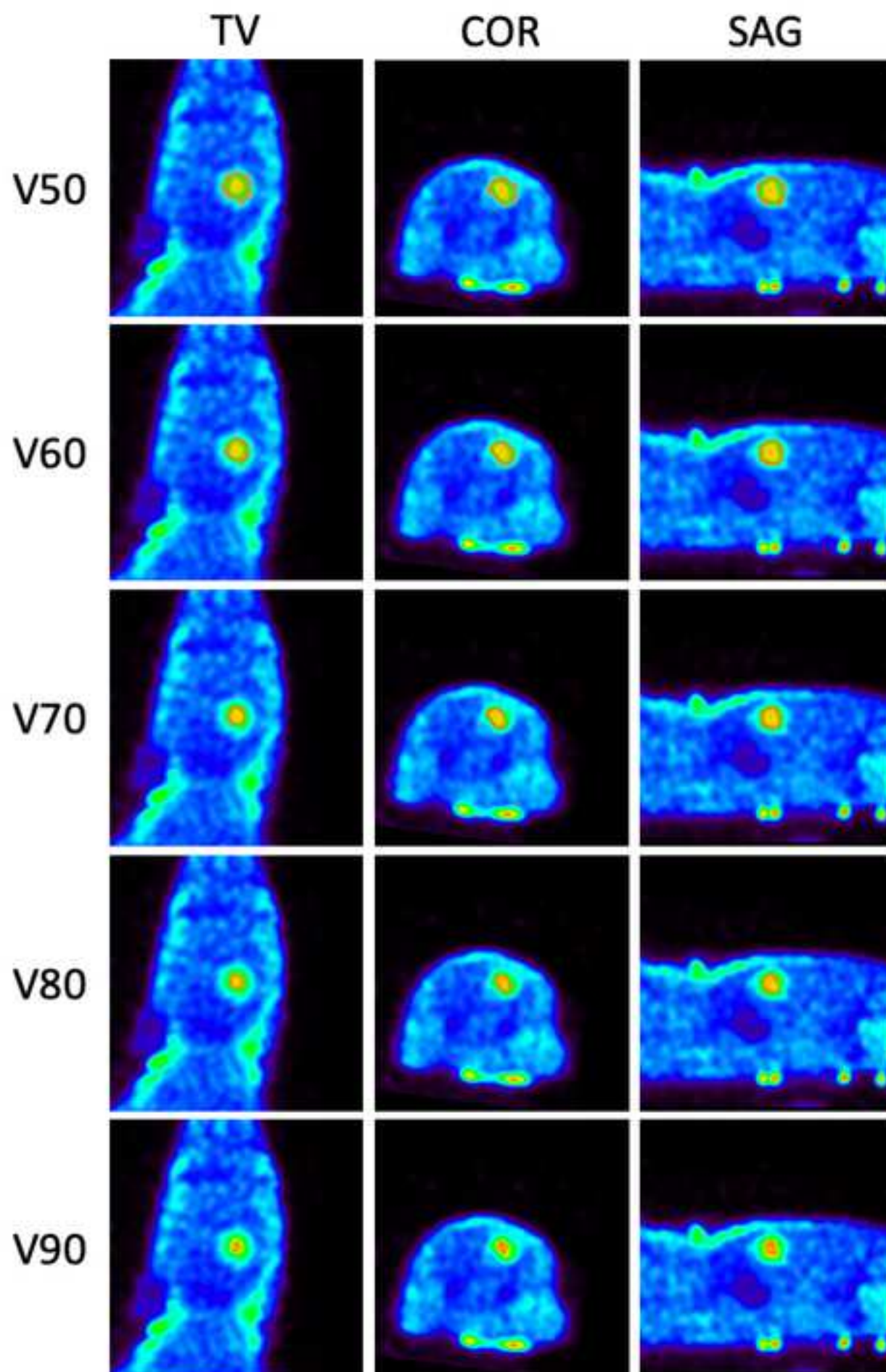


Figure 7

[Click here to access/download;Figure;Figure 7 new.jpg](#)

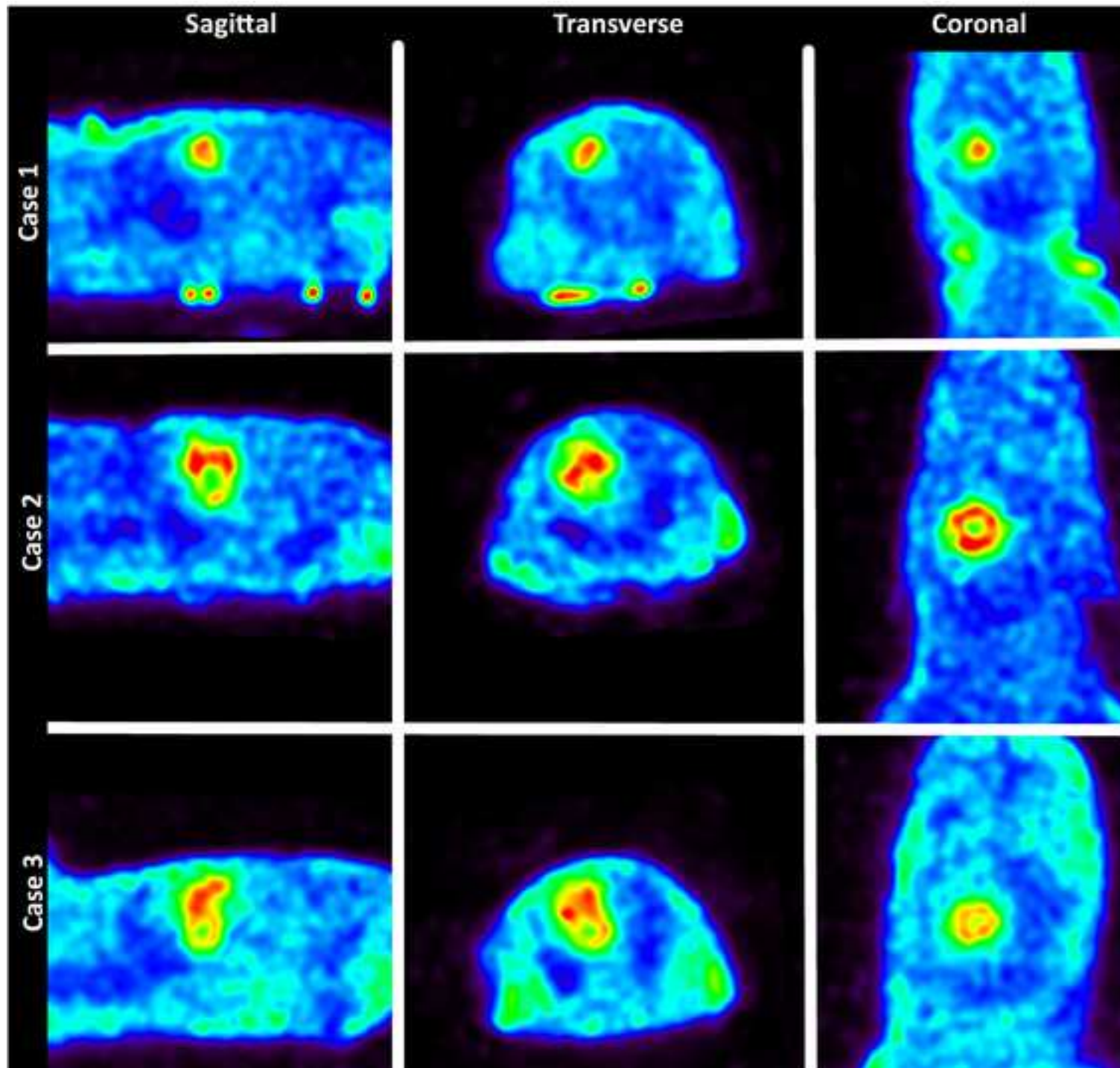




Figure 8

[Click here to access/download;Figure;Figure 8 new.jpg](#)

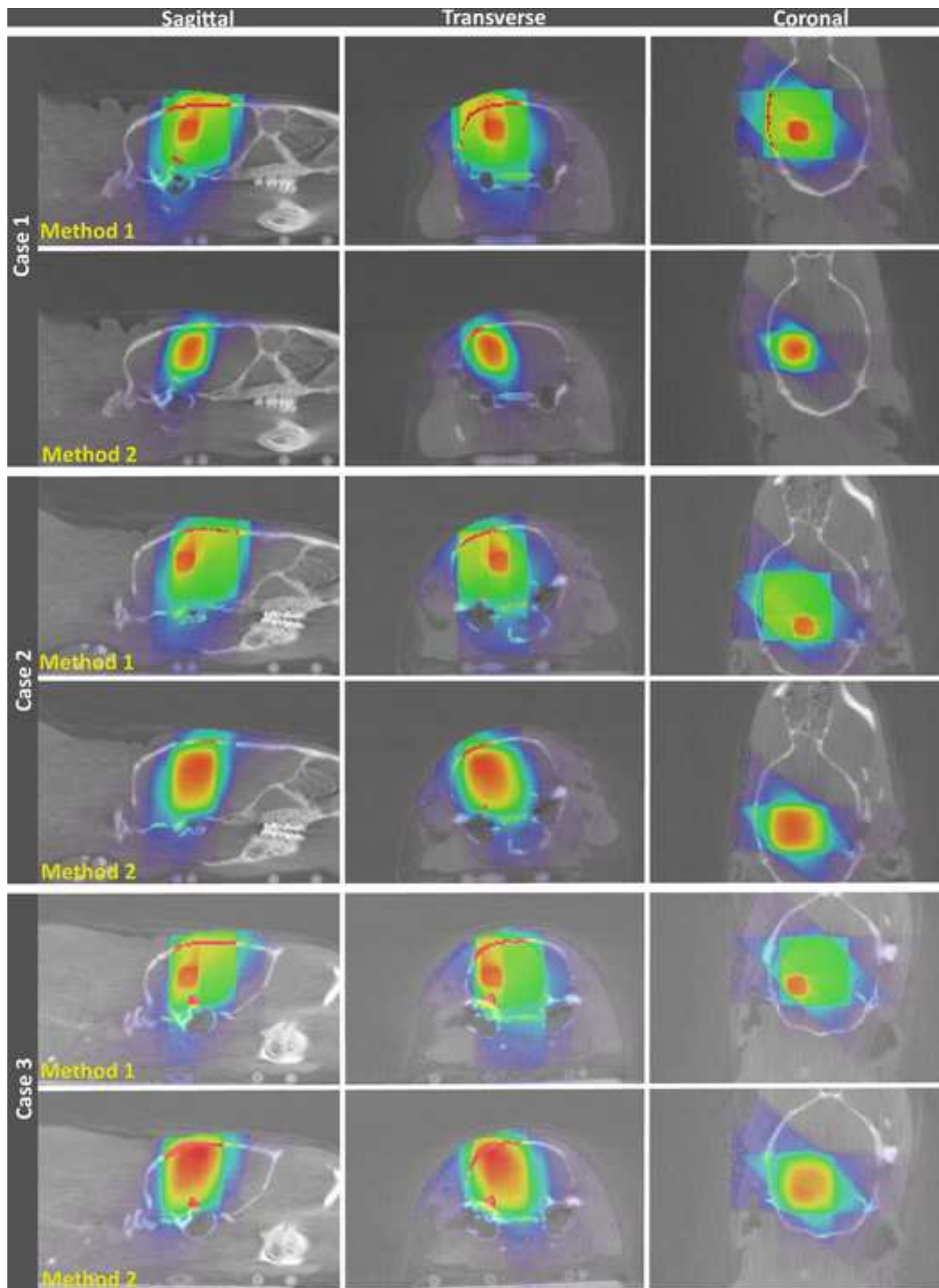
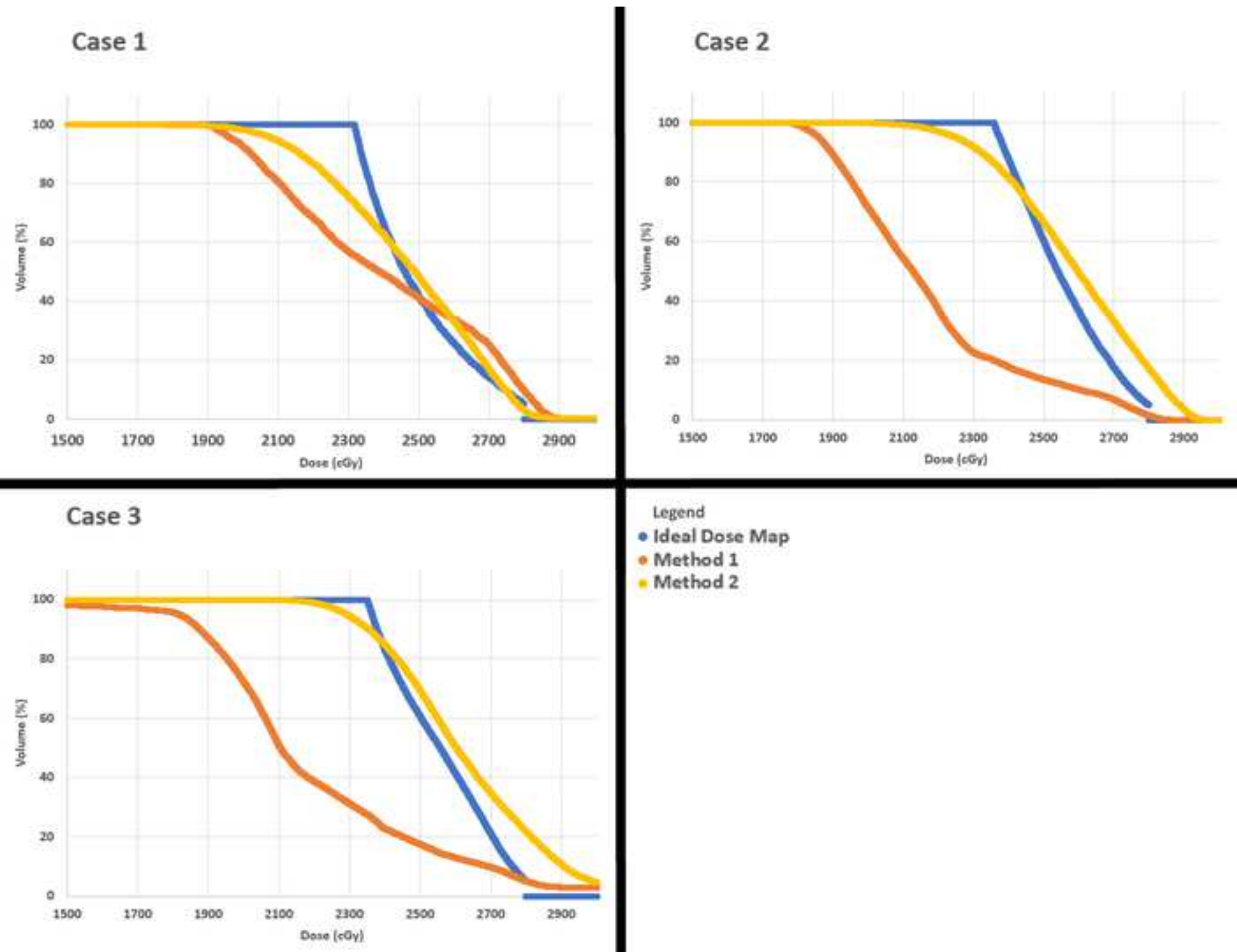
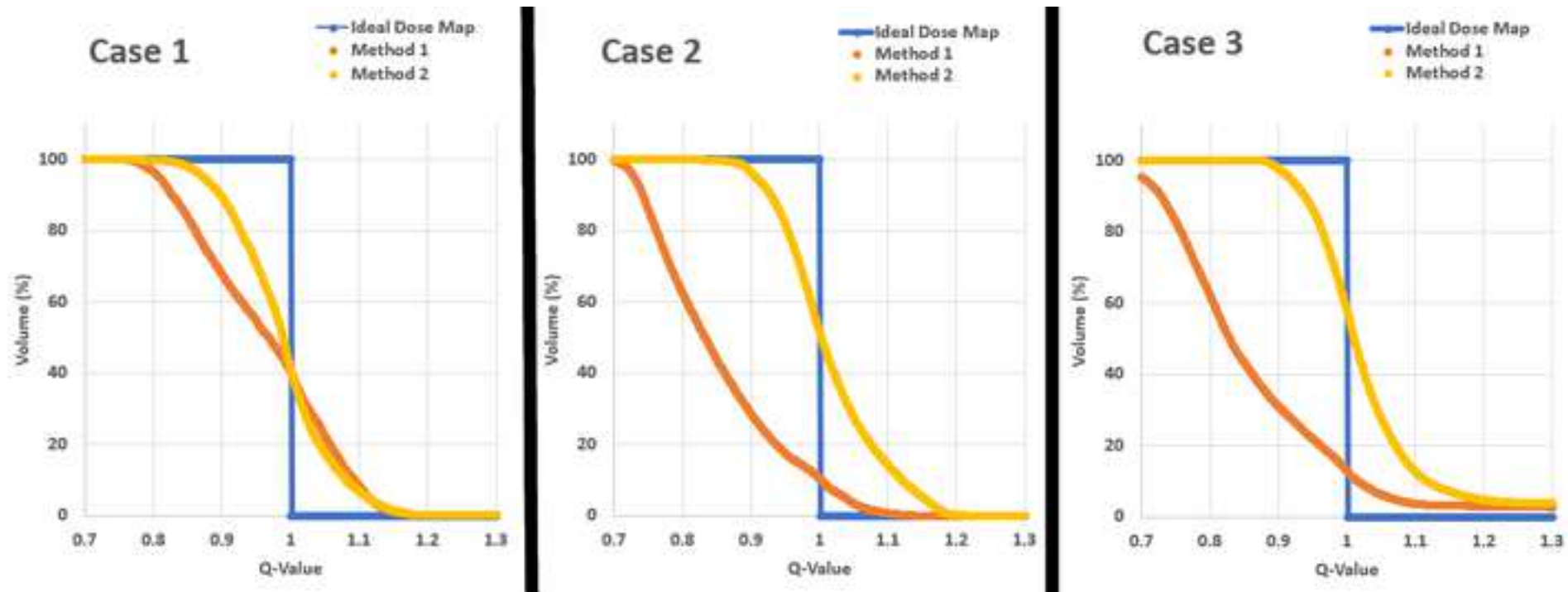


Figure 9

[Click here to access/download;Figure;Figure 9 new.jpg](#)





		Previous Method	Method 1
Tumour	Diameter	5 mm	7-8 mm
PET	Resolution (mm)	1.2	0.85
Base irradiation	Dose (cGy)	2000	2000
	Target	CE T1 tumour	CE T1 tumour
	Collimator (mm <sup>2</sup> )	5x5	10x10
	Delivery	3 non-coplanar arcs	3 non-coplanar arcs
	Couch positions	-45°, 0°, 45°	0°, -45°, -90°
Irradiation boost or dose painting	Dose (cGy)	500	800
	Target	Max PET uptake	Max PET uptake
	Collimator (mm <sup>2</sup> )	1x1	3x3
	Delivery	3 non-coplanar arcs	3 non-coplanar arcs
	Couch positions	-45°, 0°, 45°	0°, -45°, -90°



Method 2

7-8 mm

0.85

2000

V50

MVC

16 beams

0°, -45°, -90°

800

V60-V90

MVC

40 beams

0°, -45°, -90°

Couch Position				Gantry position			
0°	-	<b>20°</b>	<b>40°</b>	<b>60°</b>	80°	100°	120°
-45°	-	<b>20°</b>	<b>40°</b>	<b>60°</b>	80°	100°	120°
-90°	<b>0°</b>	<b>20°</b>	<b>40°</b>	<b>60°</b>	-	-	-

Table 3

		D90	D50	D10
Case 1	Ideal Dose Map	2336.94	2461.21	2745.63
	Method 1	2024.47	2389.75	2796.82
	Method 2	2164.21	2490.18	2747.64
Case 2	Ideal Dose Map	2391.76	2540.55	2752.56
	Method 1	1894.93	2127.86	2606.48
	Method 2	2322.11	2597.31	2848.03
Case 3	Ideal Dose Map	2377.47	2556.7	2761.38
	Method 1	1874.58	2103.78	2691.69
	Method 2	2354.03	2602.64	2907.41

Table 4

[Click here to access/download;Table;Table 4.xlsx](#) 

Q-factor	Case 1	Case 2	Case 3
Method 1	0.0898	0.1573	0.1773
Method 2	0.0572	0.057	0.0778

Name of Material/ Equipment	Company	Catalog Number
<b>Cell culture</b>		
F98 Glioblastoma Cell Line	ATCC	CRL-2397
Dulbeco's Modified Eagle Medium	Thermo Fisher Scientific	22320-030
Cell culture flasks	Thermo Fisher Scientific	178883
FBS	Thermo Fisher Scientific	10270106
L-Glutamine	Thermo Fisher Scientific	25030-032
Penicilline-Streptomycin	Thermo Fisher Scientific	15140-148
Phosphate-Buffered Saline (PBS)	Thermo Fisher Scientific	14040-224
Trypsin-EDTA	Thermo Fisher Scientific	25300-062
<b>GB Rat Model</b>		
Ball-shaped burr	Foredom	A-228
Bone Wax	Aesculap	1029754
Ethilon	Ethicon	662G/662H
Fischer F344/Ico crl Rats	Charles River	-
Insulin Syringe Microfine	Beckton-Dickinson	320924
IR Lamp	Philips	HP3616/01
Meloxicam (Metacam)	Boehringer Ingelheim	-
Micromotor rotary tool	Foredom	K.1090-22
Micropump system	Stoelting Co.	53312
Stereotactic frame	Stoelting Co.	51600
Xylocaine (1%, with adrenaline 1:200,000)	Aspen	-
Xylocaine gel (2%)	Aspen	-
<b>Animal Irradiation</b>		
Micro-irradiator	X-Strahl	SARRP
Software	X-Strahl	Muriplan
<b>Small Animal PET</b>		
[ <sup>18</sup> F]FET	Inhouse made	-
Micro-PET	Molecubes	Beta-Cube
<b>Small Animal MRI</b>		
Micro-MRI	Bruker Biospin	Pharmascan 70/16
30 G Needle for IV injection	Beckton-Dickinson	305128

PE 10 Tubing	Instech Laboratories Inc	BTPE-10
Prohance contrast agent	Bracco Imaging	-
Tx/Rx Rat Brain - Mouse Whole Body		
Volumecoil	Bruker Biospin	-
Water-based Heating Unit	Bruker Biospin	MT0125
<b>Consumables</b>		
Isoflurane	Zoetis	B506
Insulin Syringe Microfine	Beckton-Dickinson	320924
<b>Image Analysis</b>		
MATLAB	Mathworks	-
PMOD	PMOD technologies LLC	

## Comments/Description

<https://www.lgcstandards-atcc.org/products/all/CRL-2397>

75 cm<sup>2</sup>

200 mM

10,000 U/mL

0.05%

1.8 mm

<https://www.aesculapusa.com/en/healthcare-professionals/or-solutions/or-solutions-cranial-closure/hemostatic-bone-wax.html>

FS-2, 4-0, 3/8, 19 mm

1 mL, 29 G

2 mg/mL

Stoelting Stereotaxic Injector

1%, with adrenaline 1:200,000

2%

Version 4.2.0

Preclinical treatment planning system (PCTPC), version 2.2.2

PET tracer; along with Prohance: MRI/PET agent

<https://www.molecubes.com/b-cube/>

<https://www.bruker.com/products/mr/preclinical-mri/pharmascan.html>

BTPE-10, polyethylene tubing 0.011 x 0.024 in (0.28 x 60 mm), non sterile, 30 m (98 ft) spool, Instech laboratories, Inc Plymouth meeting  
279.3 mg/mL, gadolinium-contrast agent (along with [ $^{18}\text{F}$ ]FET: MRI/PET agent)

40 mm diameter

Anesthesia

1 mL, 29 G

Version R2019b

Preclinical and molecular imaging software





g PA USA- (800) 443-4227- <http://www.instechlabs.com>

Dear editor

Dear reviewer

Thank you for giving feedback and constructive criticism on our manuscript, JoVE62560 “PET-based dose painting radiation therapy strategy in a glioblastoma rat model using the Small Animal Radiation Research Platform”. We addressed your comment in the document below.

Kind regards

Sam Donche

## Answer Revision: PET-based dose painting radiation therapy strategy in a glioblastoma rat model using the Small Animal Radiation Research Platform (JoVE62560)

### Editorial comments

1. Please take this opportunity to thoroughly proofread the manuscript to ensure that there are no spelling or grammar issues.

[The manuscript has been proofread by the co-authors.](#)

2. Please revise the following lines to avoid previously published work: 52-55, 59-61, 82-89, 94-107, 116-120, 122-124, 130-133, 139-148, 157-158, 178-179, 185-187, 193-196, 197-198.

[Small changes have been made to lines 52-55, 59-61, 82-89, 94-107.](#)

3. Please revise the text to avoid the use of any personal pronouns (e.g., "we", "you", "our" etc.).

[The manuscript has been revised for personal pronouns.](#)

4. JoVE cannot publish manuscripts containing commercial language. This includes trademark symbols (™), registered symbols (®), and company names before an instrument or reagent. Please remove all commercial language from your manuscript and use generic terms instead. All commercial products should be sufficiently referenced in the Table of Materials. For example: Prohance, etc.

[Company names have been removed from the manuscript.](#)

5. Line 136-137: Please include the size of the suture used.

[Suture specifications are now added to the manuscript \(see lines 199-201\):](#)

[“Withdraw the syringe slowly and close the hole in the skull with bone wax. Suture the skin \(polyamide 6, thickness 4-0\) and inject meloxicam subcutaneously \(1 mg/kg, 2 mg/mL\).”](#)

6. Line 139-148: Please ensure that all text in the protocol section is written in the imperative tense as if telling someone how to do the technique (e.g., “Do this,” “Ensure that,” etc.). The actions should

be described in the imperative tense in complete sentences wherever possible. Avoid usage of phrases such as “could be,” “should be,” and “would be” throughout the Protocol. Any text that cannot be written in the imperative tense may be added as a “Note.” However, notes should be concise and used sparingly. Please include all safety procedures and use of hoods, etc.

Small changes have been made throughout the manuscript.

7. Line 288/ 293: Please number the subheading (e.g., 6.1 Dose- Volume histogram) and renumber the following steps (e.g., 6.1.1., 6.1.2, etc.).

The subheading and following steps have been renumbered.

8. Please include a one-line space between each protocol step and highlight up to 3 pages of the Protocol (including headings and spacing) that identifies the essential steps of the protocol for the video, i.e., the steps that should be visualized to tell the most cohesive story of the Protocol. Remember that non-highlighted Protocol steps will remain in the manuscript, and therefore will still be available to the reader.

A one-line space is now included between each protocol step.

9. Lines 347-378: Please use the same font as the manuscript text. Remove the italics.

The font has been adjusted and the italics have been removed.

10. Please include modifications/ troubleshooting of the technique and the limitations of the technique.

A section with study limitations has been added to the Discussion (lines 561-566): “This study also has some limitations. For the experiments described in this manuscript, the most commonly used amino acid PET tracer [<sup>18</sup>F]FET was used. When using other PET tracers to guide radiation treatment, the semi-automatic workflow should be properly examined because coregistration might be less accurate. Also, the impact of using a different voxel size for PET and/or MRI on treatment planning and dose delivery should be further investigated.”

11. Please do not use the &-sign or the word “and” when listing authors in the reference section. Authors should be listed as last name author 1, initials author 1, last name author 2, initials author 2, etc. Title case and italicize journal titles and book titles. Do not use any abbreviations. Article titles should start with a capital letter and end with a period and should appear exactly as they were published in the original work, without any abbreviations or truncations.

This has been modified in the Reference section.

12. Please sort the Table of Materials in alphabetical order.

The order has been adjusted.

# Answer Revision: PET-based dose painting radiation therapy strategy in a glioblastoma rat model using the Small Animal Radiation Research Platform (JoVE62560)

## Reviewers' comments

### Reviewer #1

#### Major concerns

They use two different methods but do not describe the rational of using two methods in the introduction section.

In this paper, an *in silico* study is presented to compare two methodologies for [ $^{18}\text{F}$ ]-fluoro-ethyl-L-tyrosine ([ $^{18}\text{F}$ ]FET) PET-based dose painting in a GB rat model<sup>20-22</sup> using a small animal radiation research platform: (1) sub-volume boosting using predefined beam sizes and (2) dose painting using a motorised variable collimator where jaw dimensions are modified based on the PET tracer uptake in the tumour volume.

This is now added to the Introduction of the manuscript (lines: 108-112).

Method 1 is very similar to the previously published methodology (see reference 20-22) with a few adjustments (see Table 2). However, in contrast to the previously published methodology, most of the process is automated using an in-house developed MATLAB code. Rational behind these adjustments:

- The tumours were bigger because we wanted more tumour heterogeneity to be visible on PET and MR imaging. This results in a bigger challenge for dose painting.
- Our PET system was upgraded from a resolution of 1.2 mm to 0.85 mm. This will also result in more observed tumour heterogeneity.
- The size of the collimator for both base irradiation and boosting had to be increased due to the increased tumour size. Also, an extra margin was incorporated to account for the extra microscopic tumour infiltration.
- Arcs were defined at couch positions 0°, -45° and -90° instead of -45°, 0°, 45° because the tumour is located in the right hemisphere. This way less normal tissue will be irradiated.

Method 2 consists of a more sophisticated method where a series of isocentres and jaw dimension for the motorised variable collimator will be determined based on the [ $^{18}\text{F}$ ]FET uptake (see Figure 5).

For V50, 16 beams were defined along the arcs at couch positions 0°, -45° and -90°. A base radiation dose of 20 Gy was divided over these 16 beams, resulting in 125 cGy per beam.

For V60-V90, 40 beams were defined along the arcs at couch positions 0°, -45° and -90°. The boost dose of 8 Gy was divided over these 40 beams, resulting in 20 cGy per beam.

Also, for the PET tracer used, I don't see why FET was chosen. Please provide some explanation for using this specific radiotracer. Authors already used other tracers like FAZA for hypoxia. Do they believe that the new methods described here are well suited to any other "metabolic" imaging.

[ $^{18}\text{F}$ ]-fluoro-ethyl-L-tyrosine ([ $^{18}\text{F}$ ]FET) is a PET tracer often used in neuro-oncology because of its ability to detect brain tumours (<https://doi.org/10.1093/neuonc/nos300>). FET is an artificial amino acid that is internalised in tumoral cells but not incorporated into cell proteins. [ $^{18}\text{F}$ ]FET uptake corresponds with cell proliferation rate, tumour cell density and angiogenesis

(<https://doi.org/10.1007/s11060-008-9551-3>). As this is the most used oncologic brain PET tracer in our institute, this radiotracer was chosen to evaluate our new workflow.

This is now added to the manuscript at the end of the Introduction (lines: 112-116).

The workflow has not been tested with other PET tracers yet. This will be further evaluated in the future. Therefore, the following sentence has also been added to the manuscript (lines: 561-565): "This study also has some limitations. For the experiments described in this manuscript, the most commonly used amino acid PET tracer [<sup>18</sup>F]FET was used. When using other PET tracers to guide radiation treatment, the semi-automatic workflow should be properly examined because coregistration might be less accurate."

The duration for each method is not discussed. Line 410, they mention "about 80min". Is the duration similar for the two methods? if motorized variable collimator has to be used, does it take time?

This was indeed not so clear in the manuscript.

While conventional (i.e. completely manual) preclinical treatment planning, including multimodal imaging, can require up to 180 minutes, this time could be reduced to about 80 minutes with both semi-automatic methods presented in this manuscript.

This has now been modified in the manuscript (lines: 539-541).

We assume that dose delivery might be slightly slower when using a motorised variable collimator to switch between beam positions and to adjust the jaw dimensions for each individual beam.

This has also added to the manuscript (lines: 552-554).

For the methodology, on line255: "a 10\*10collimator is used". It is well suited since tumor diameter equal of around 8mm were chosen. How should user manage if smaller tumor volumes are desired? or tumor volume greater than 8mm?

The SARRP comes with multiple fixed collimators: 1 mm diameter, 3 mm x 3 mm, 5 mm x 5 mm and 10 mm x 10 mm. So, when smaller tumour sizes have to be irradiated, the appropriate (fixed-sized) collimator should be selected. Our research group likes to incorporate an extra margin around the tumour to account for microscopic tumour infiltration. The animal's welfare must be considered when using tumour volumes larger than 10 mm.

The following sentence was added to the manuscript (line 354-356):

"When smaller tumour sizes need to be irradiated, appropriate collimators should be applied (e.g. a 5 x 5 mm collimator). The animal's welfare must be considered when using tumour volumes larger than 10 mm."

I would also need more information to link the supplementary dose in the boost with the biology of the tumor. Here a 2.8 Gy dose is used in the most FET avid region. How was chosen a 0.8 Gy boost?

In this experiment, we chose to dose paint between a dose of 20 Gy and 28 Gy within the tumour target. The clinical used dose is 30 x 2 Gy. As carrying out 30 fractions would be impossible to perform, the radiation therapists at our hospital proposed to deliver one dose of 20 Gy based on the biologically effective dose and biological equivalent dose. In a similar manner, the boost of 8 Gy was chosen to have enough tumour control probability and keep the risk of normal tissue complications low (normal tissue complications probability).

For DHV data, they compare to an ideal dose map. How was calculated this "ideal" dose?

The ideal dose was calculated using Equation 1. This equation is a linear interpolation between minimum dose and maximum dose, proportional varying between the minimum PET intensity and maximum PET intensity within the target volume.

This has now been clarified in the manuscript (lines: 405-408).

For radiation treatment planning, did they studied the impact of using other image resolution (from MRI or PET) on the ultimate tumor and sub-volume automatic segmentation.

The impact of using other image resolutions on the ultimate tumour and sub-volume automatic segmentation was not evaluated. This could indeed be studied in further research.

The following sentence was added to the discussion (lines: 562-563):

“This study also has some limitations, the impact of using other image resolutions for PET and/or MRI on treatment planning and dose delivery should be further investigated.”

In the discussion, they mention that a lower dose deposition could be achieved using MVC. I believe that more quantitative data would make the conclusion more evident.

We agree with the reviewer that more quantitative data would make the conclusion more evident. However, we believe that our data shows that the use of the motorized variable collimator results in a more accurate dose delivery in the tumour by using the quantitative Q-factor and less dose on the normal tissue, which is illustrated in Figure 7 and Table 4.

Minor concerns

line61: ref 6 does not seem to be appropriate.

Ref 6 was replaced by two different references.

Von Neubeck, C., Seidlitz, A., Kitzler, H. H., Beuthien-Baumann, B., Krause, M. Glioblastoma multiforme: Emerging treatments and stratification markers beyond new drugs. *Br. J. Radiol.* **88**, (2015).

Mann, J., Ramakrishna, R., Magge, R., Wernicke, A. G. Advances in radiotherapy for glioblastoma. *Front. Neurol.* **8**, 1–11 (2018).

line 164: non-isotropic voxels are obtained. Authors could have rather applied a lower in plane resolution but decreased the slice thickness.

We indeed used our default MRI protocol for T1- and T2-weighted imaging, where we prefer a higher in-plane resolution with a larger slices thickness to obtain a sufficient signal-to-noise ratio (with acceptable acquisition times). However, we fully agree with the reviewer that a reduced slice thickness could be used when compensated by a lower in-plane resolution to obtain the same signal-to-noise ratio.

As already mentioned above, we didn't evaluate the impact of using other image resolutions on treatment planning outcome and therefore the following sentence was added to the discussion (lines: 561-565): “This study also has some limitations. For the experiments described in this manuscript, the most commonly used amino acid PET tracer [<sup>18</sup>F]FET was used. When using other PET tracers to guide radiation treatment, the semi-automatic workflow should be properly examined because coregistration might be less accurate. Also, the impact of using a different voxel size for PET and/or MRI on treatment planning and dose delivery should be further investigated.”

line 191: a 0.4mm reco is used. I don't understand why, it is below the actual resolution of 18F compounds. It will then be reprocessed to reach a final resolution of 0.275mm

PET imaging was done on a Molecubes B-Cube system. This system has a sub-mm spatial resolution and using the manufacturer's reconstruction software, the images can be reconstructed with a voxels size of 0.4 mm or 0.8 mm. For this study, we selected the higher spatial resolution of 0.4 mm.

line165; 191 and 204: use the same unit (either mm or  $\mu\text{m}$ ).

This was adapted in the manuscript.

line 214. " of 1.54 mm. And can be calculated by". A word is missing ?

As a result of a comment of another reviewers, this section (4.2) has been modified.

---



## Answer Revision: PET-based dose painting radiation therapy strategy in a glioblastoma rat model using the Small Animal Radiation Research Platform (JoVE62560)

### Reviewers' comments

#### Reviewer #2

##### Minor Comments

1.2.7 Although this will be site specific, rats involved in similar tumour surgeries at our site receive another injection of Metacam subcutaneously after recovery from surgery to reduce inflammation and pain on days 1 and 2, post-operatively. We are also required to maintain a daily health status log with similar endpoints (20% weight loss and/or deterioration of normal behaviour).

An injection of Metacam was at our institute indeed only given post-operatively on the day of the surgery. The addition of two extra injections on day 1 and day 2 post-inoculation could indeed be considered for future experiments.

During our experiments a daily health status log was also kept (see 1.2.7.). This has been better clarified in section 1.2.7.

2.3/2.4 Define acronyms: TR, TE, TA. Is the T1-weighted sequence also a spin-echo sequence (FSE/RARE)? How many slices are acquired for each sequence?

The acronyms TR, TE and TA are now defined in the manuscript. Both T<sub>1</sub> and T<sub>2</sub>-weighted images are spin-echo sequences and are composed of 30 slices. This information has also been added to the manuscript in section 2.3 (lines: 228-231).

2.6 How often do you monitor tumor growth (every 2-3 days)? If done carefully, tumour growth can be quite predictable. Do you have an estimate for number of days post-inoculation you have a 7-8 mm tumour?

As stated by the reviewer, tumour growth can be quite predictable. Using MR imaging, the tumour usually reaches a size of approximately 5 mm, nine days post inoculation. Then, MR imaging was indeed performed every 2-3 days until the required tumour size is reached. For our experiments, a size of 7-8 mm was desired. This was generally obtained around 12 days post inoculation.

Section 2.6 has been slightly modified to include this information: "When the tumour reaches a diameter of 7 to 8 mm, usually observed 12 days after inoculation, the animal is selected for therapy."

3.2 Define [<sup>18</sup>F]FET and what it measures.

[<sup>18</sup>F]-fluoro-ethyl-L-tyrosine ([<sup>18</sup>F]FET) is a PET tracer often used in neuro-oncology because of its ability to detect brain tumours<sup>1</sup>. FET is an artificial amino acid that is internalised in tumoral cells but not incorporated into cell proteins. [<sup>18</sup>F]FET uptake corresponds with cell proliferation rate, tumour cell density and angiogenesis<sup>2</sup>.

The following sentences were added to the introduction of the manuscript (lines: 112-115)

"[<sup>18</sup>F]FET is a PET tracer often used in neuro-oncology because of its ability to detect brain tumours<sup>1</sup>. [<sup>18</sup>F]FET is an artificial amino acid that is internalised in tumoral cells but not

incorporated into cell proteins. [<sup>18</sup>F]FET uptake corresponds with cell proliferation rate, tumour cell density and angiogenesis<sup>2</sup>.”

1. Hutterer, M. *et al.* FET PET: a valuable diagnostic tool in neuro-oncology, but not all that glitters is glioma. *Neuro. Oncol.* **15**, 341–351 (2013).
2. Stockhammer, F., Plotkin, M., Amthauer, H., Landeghem, F. K. H. & Woiciechowsky, C. Correlation of F-18-fluoro-ethyl-tyrosin uptake with vascular and cell density in non-contrast-enhancing gliomas. *J. Neurooncol.* **88**, 205–210 (2008).

### 3.3 What is used for the MRI/PET agent? [<sup>18</sup>F]FET and Prohance?

The tumour is indeed visualised using two agents. [<sup>18</sup>F]FET and a gadolinium-containing contrast agent (Prohance) are used to visualize the tumour on PET and MRI, respectively.

### 3.3 Is there a reason you can't use the heated blanket used for the MRI tumor checks?

A heated blanket can be used and was used during MR imaging to monitor tumour growth. However, it could not be used during the multimodal imaging session for treatment planning due to the design of the in-house made multimodality bed, which was used for this purpose. This multimodality bed was made to move the animal smoothly from one imaging device to another, while minimizing animal motion. To maintain body temperature, the animal was wrapped in bubble wrap and to further avoid animal motion the heated blanket was not placed on the animal during MRI.

### 3.4 Optimal PET reconstruction would be system-dependent. Describe PET system used in this experiment.

The PET system in this article is a Beta-cube (Molecubes, <https://www.molecubes.com/b-cube/>). This system has a field of view (FOV) of 130 mm x 72 mm and a spatial resolution of 0.85 mm.

More details related to the PET-system are now added to section 3.4 of the manuscript: “Note, that a dedicated PET scanner for laboratory animal imaging was used with an axial field of view of 130 mm and a bore diameter of 72 mm. This system provides sub-mm (0.85 mm) spatial resolution.”

### 3.5 Define MRI contrast agent (Prohance?)

Prohance (Bracco Imaging, 279.3 mg/mL) is a gadolinium-based MRI contrast agent. The ‘active’ molecule is gadoteridol. To meet the requirements of the journal, the commercial product name ‘Prohance’ had to be deleted and replaced by (lines 223-224):

“Inject a gadolinium-containing contrast agent (0.4 mL/kg) through an intravenously placed tubing in the lateral tail vein.”

### 4.2 I don't understand the origin of this equation. Why is FWHM = 1 mm and pixel dimension 0.275 mm? Please cite and/or explain.

To increase readability, we modified section 4.2 of the manuscript to: “Import the converted images into MATLAB and filter the PET image with a Gaussian filter using a Full Width Half Max (FWHM) of 1 mm.”

The origin of the equation in section 4.2 comes from the MATLAB function *imgaussfilter3* that is used to perform Gaussian filtering. This function requires as input the standard deviation of the Gaussian curve instead of the more commonly used Full Width Half Maximum value.

In our previously published workflow, the images were filtered with a Gaussian filter with a FWHM-value of 1 mm. We didn't want the PET filtration step to vary between the previously described method. This FWHM-value also matches more or less with the spatial resolution of our PET imaging system.

#### 4.6 What type of transformation does SPM perform? Rigid? Affine? Will mutual information suffice for other PET tracers?

The coregistration within SPM consists of rigid-body transformations. This has now been clarified into the manuscript in section 4.5.

The two described methods have only been validated using [ $^{18}\text{F}$ ]FET. Brain tumour uptake of [ $^{18}\text{F}$ ]FET is quite specific, so we believe that mutual information might also work other PET tracers. However, this has not been investigated yet. Therefore, the following sentence was added to the manuscript (lines 553-555):

“For these experiments the most commonly used amino acid PET tracer [ $^{18}\text{F}$ ]FET was used. When using other PET tracers, the workflow should be properly examined.”

#### 5. Can you describe the rationale behind the two radiation treatment planning methods?

In this paper, an *in silico* study is presented to compare two methodologies for [ $^{18}\text{F}$ ]-fluoro-ethyl-L-tyrosine ([ $^{18}\text{F}$ ]FET) PET-based dose painting in a GB rat model<sup>20-22</sup> using a small animal radiation research platform: (1) sub-volume boosting using predefined beam sizes and (2) dose painting using a motorised variable collimator where jaw dimensions are modified based on the PET tracer uptake in the tumour volume.

This is now added to the Introduction of the manuscript (lines: 108-112).

Method 1 is very similar to the previously published methodology (see reference 20-22) with a few adjustments (see Table 2). However, in contrast to the previously published methodology, most of the process is automated using an in-house developed MATLAB code. Rationale behind these adjustments:

- The tumours were bigger because we wanted more tumour heterogeneity to be visible on PET and MR imaging. This results in a bigger challenge for dose painting.
- Our PET system was upgraded from a resolution of 1.2 mm to 0.85 mm. This will also result in more tumour heterogeneity.
- The size of the collimator for both base irradiation and boosting had to be increased due to the increased tumour size. Also, an extra margin was incorporated to account for the extra microscopic tumour infiltration.
- Arcs were defined at couch positions 0°, -45° and -90° instead of -45°, 0°, 45° because the tumour is located in the right hemisphere. This way less normal tissue will be irradiated.

Method 2 consists of a more sophisticated method where a series of isocentres and jaw dimension for the motorised variable collimator will be determined based on the [ $^{18}\text{F}$ ]FET uptake (see Figure 5).

For V50, 16 beams were defined along the arcs at couch positions 0°, -45° and -90°. A base radiation dose of 20 Gy was divided over these 16 beams, resulting in 125 cGy per beam.

For V60-V90, 40 beams were defined along the arcs at couch positions 0°, -45° and -90°. The boost dose of 8 Gy was divided over these 40 beams, resulting in 20 cGy per beam.

#### 5.6 Can you show a figure with the isocontours for V50, V60, V70, V80, and V90?

An image is added (Figure 10) to the manuscript that show the V50, V60, V70, V80 and V90 contours.

